

AD-A071 447

MASSACHUSETTS INST OF TECH CAMBRIDGE DEPT OF MATERIA--ETC F/G 20/12  
ELECTRONIC CHARACTERISTICS OF III-V COMPOUNDS.(U)  
MAY 79 H C GATOS

F19628-77-C-0060

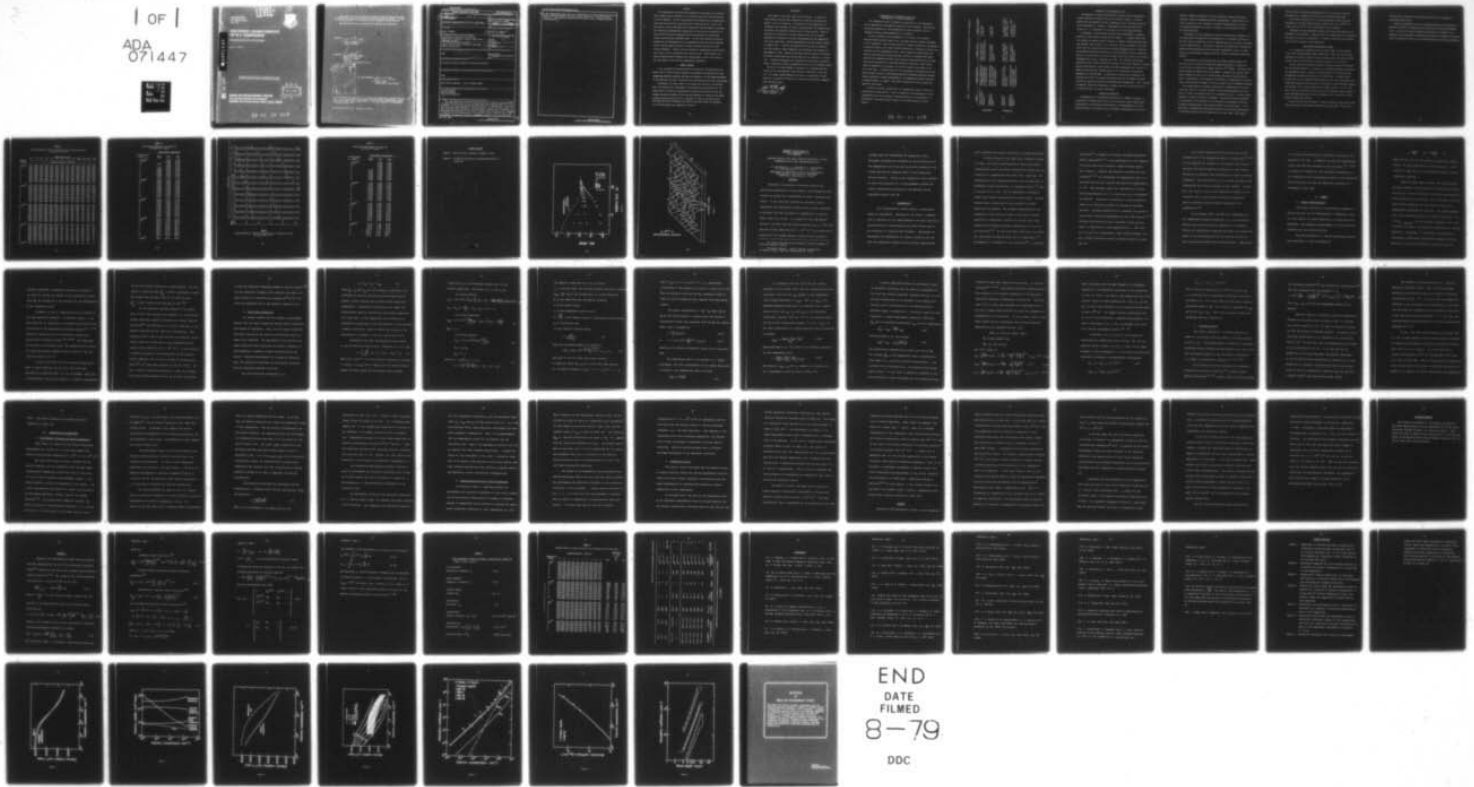
UNCLASSIFIED

RADC-TR-79-95

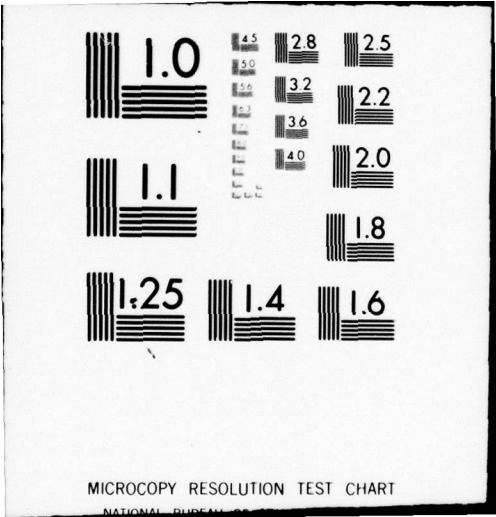
NL

| OF |

ADA  
071447



END  
DATE  
FILMED  
8-79  
DDC



MICROCOPY RESOLUTION TEST CHART

NATIONAL BUREAU OF STANDARDS-1963-A

**LEVEL** #



**RADC-TR-79-95**  
Final Technical Report  
May 1979

# **ELECTRONIC CHARACTERISTICS OF III-V COMPOUNDS**

**Massachusetts Institute of Technology**

Harry C. Gatos

**A071447**

**APPROVED FOR PUBLIC RELEASE; DISTRIBUTION UNLIMITED**

**DDC FILE COPY**

**DDC**  
**RECEIVED**  
**JUL 20 1979**  
**RESOLV**  
**A**

**ROME AIR DEVELOPMENT CENTER**  
**Air Force Systems Command**  
**Griffiss Air Force Base, New York 13441**

**79 07 19 018**



This report has been reviewed by the RADC Information Office (OI) and is releasable to the National Technical Information Service (NTIS). At NTIS it will be releasable to the general public, including foreign nations.

RADC-TR-79-95 has been reviewed and is approved for publication.

APPROVED:

*John F. Kennedy*  
JOHN K. KENNEDY  
Contract Monitor

APPROVED:

*Robert M. Barrett*  
ROBERT M. BARRETT  
Director  
Solid State Sciences Division

Accession For	
NTIS GRA&I	<input checked="" type="checkbox"/>
DDC TAB	<input type="checkbox"/>
Unannounced Justification	<input type="checkbox"/>
By	
Distribution/	
Availability Codes	
Dist	Avail and/or special
A	

FOR THE COMMANDER:

*John P. Huss*  
JOHN P. HUSS  
Acting Chief, Plans Office

If your address has changed or if you wish to be removed from the RADC mailing list, or if the addressee is no longer employed by your organization, please notify RADC (ESM), Hanscom AFB MA 01731. This will assist us in maintaining a current mailing list.

Do not return this copy. Retain or destroy.



UNCLASSIFIED

SECURITY CLASSIFICATION OF THIS PAGE (When Data Entered)

REPORT DOCUMENTATION PAGE		READ INSTRUCTIONS BEFORE COMPLETING FORM
1. REPORT NUMBER <b>18</b> RADC TR-79-95	2. GOVT ACCESSION NO.	3. RECIPIENT'S CATALOG NUMBER <b>9</b>
4. TITLE (and Subtitle) <b>6</b> ELECTRONIC CHARACTERISTICS OF III-V COMPOUNDS	5. TYPE OF REPORT & PERIOD COVERED Final Technical Report 1 January 77 - 30 September 78	
7. AUTHOR(s) <b>10</b> Harry C. Gatos	6. PERFORMING ORG. REPORT NUMBER N/A	
9. PERFORMING ORGANIZATION NAME AND ADDRESS Massachusetts Institute of Technology Department of Materials Science & Engineering Cambridge MA 02139	8. CONTRACT OR GRANT NUMBER(s) <b>15</b> F19628-77-C-0060	
11. CONTROLLING OFFICE NAME AND ADDRESS Deputy for Electronic Technology (RADC/ESM) Hanscom AFB MA 01731	10. PROGRAM ELEMENT, PROJECT, TASK AREA & WORK UNIT NUMBERS 61102F 2306J120 <b>12</b> 76p.	
14. MONITORING AGENCY NAME & ADDRESS (if different from Controlling Office) Same <b>16</b> 2306	12. REPORT DATE <b>11</b> May 1979	
	13. NUMBER OF PAGES 72	
	15. SECURITY CLASS. (of this report) UNCLASSIFIED	
	15a. DECLASSIFICATION/DOWNGRADING SCHEDULE N/A	
16. DISTRIBUTION STATEMENT (of this Report) Approved for public release; distribution unlimited		
17. DISTRIBUTION STATEMENT (of the abstract entered in Block 20, if different from Report) Same		
18. SUPPLEMENTARY NOTES RADC Project Engineer: John K. Kennedy (ESM)		
19. KEY WORDS (Continue on reverse side if necessary and identify by block number) Gallium Arsenide Indium Phosphide Electronic Properties		
20. ABSTRACT (Continue on reverse side if necessary and identify by block number) Our experimental and theoretical program has been aimed at the development of approaches and methods for the reliable electronic characterization of III-V compounds. We have investigated the determination of compositional, structural and electronic characteristics of GaAs and InP on a macro- and micro-scale. We have developed novel theoretical and experimental techniques for obtaining two-dimensional microprofiles of the carrier concentration in GaAs and InP (scanning IR absorption) and microprofiles of the minority carrier characteristics (SEM-EBIC mode). We have also developed convenient methods for the determination		

DD FORM 1 JAN 73 1473

UNCLASSIFIED

SECURITY CLASSIFICATION OF THIS PAGE (When Data Entered)

4109 463

5073

of the compensation ratio and total concentration of ionized impurities which is based on electron mobility and free carrier absorption. Finally, we have initiated a comprehensive characterization study of InP in conjunction with crystal growth.

## Preface

Our experimental and theoretical program has been aimed at the development of approaches and methods for the reliable electronic characterization of III-V compounds. We have investigated the determination of compositional, structural and electronic characteristics of GaAs and InP on a macro- and micro-scale. We have developed novel theoretical and experimental techniques for obtaining two-dimensional microprofiles of the carrier concentration in GaAs and InP (scanning IR absorption) and microprofiles of the minority carrier characteristics (SEM-EBIC mode). We have also developed convenient methods for the determination of the compensation ratio and total concentration of ionized impurities which is based on electron mobility and free carrier absorption. Finally, we have initiated a comprehensive characterization study of InP in conjunction with crystal growth. Unfortunately, as a unique characterization framework was being brought to bear on the study of InP, the support of the work was unexpectedly terminated.

## GENERAL REMARKS

It is now generally accepted within the scientific and engineering community that to insure further progress in processing and application of semiconducting materials extensive work must be carried out on the characterization of the materials in direct correlation with crystal growth and device processing.

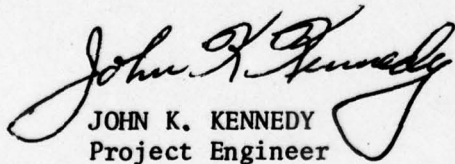
Accordingly, the first stage of our program was devoted to the development of theoretical and experimental characterization approaches and to the design and construction of experimental facilities which would fill the gap between the existing needs and the available methods for practical and highly reliable characterization of III-V compounds on a macro- and micro-scale. The characterization techniques and methods developed within the framework of the present grant are summarized in Table 1.



## EVALUATION

This report is the final report on the contract. It covers research done on the Electronic properties of GaAs and InP during the period 1 Jan 77 to 30 Sep 78. The objective of the research was to investigate and determine on a macro- and micro-scale the compositional, structural, and electronic characteristics of GaAs and InP. Rigorous theoretical calculations of electron mobility and of free carrier absorption as a function of carrier concentration and the compensation ratio were carried out, verified experimentally and the results reduced to tabular form. A reliable determination of free carrier concentration and testing of sample homogeneity was developed using transport in high magnetic fields. Apparatus and theory were developed for profiling of carrier concentration and ionized impurities by scanning I.R. absorption. A method and apparatus were developed for profiling of diffusion length, lifetime and surface recombination velocity of the SEM-EBIC method.

The work is of value because it provides basic knowledge and techniques for the investigation of the electronic properties of GaAs and InP. An in-depth understanding of the electronic properties of these materials is essential for their use in optical and electronic communications and ECM systems.

  
JOHN K. KENNEDY  
Project Engineer

DETERMINATION OF COMPENSATION RATIO AND  
CONCENTRATION OF IONIZED IMPURITIES

The compensation ratio and impurity concentration are the parameters of key importance in semiconductor application and technology. Nevertheless, the existing methods for the determination of these parameters in III-V compounds have been either impractical or unreliable.

We have succeeded in the development of an accurate and convenient characterization approach based on low- and high-frequency transport phenomena in III-V compounds. Thus, we have carried out rigorous theoretical calculations of electron mobility and of free carrier absorption as a function of carrier concentration and the compensation ratio. These theoretical results have been verified experimentally and they have been utilized to establish the tables from which the compensation ratio can be directly obtained from carrier concentration and from mobility or infrared absorption coefficient. These tables, which are appended to this report, are far more accurate than those in use up to this time. A detailed account of the experimental and theoretical treatment for GaAs is given in the enclosed preprint on "Electron Mobility and Free Carrier Absorption in GaAs; Determination of the Compensation Ratio", (Journal of Applied Physics, in press). The results obtained with InP are being prepared for publication.

It has been recently reported that the compensating centers in GaAs are associated with point defects. Thus, our method for the determination of the compensation ratio can be used as a convenient means for the assessment of the quality of the material with respect to the overall density of point defects.

79 07 19 018

TABLE 1. Techniques and Methods Developed for the Characterization of III-V Compounds

METHOD	CHARACTERIZATION	PRESENT STATUS	MATERIAL STUDIED
MACROSCALE	Electron Mobility & Free Carrier Absorption	Theory developed for n-type GaAs & InP & verified experimentally	n-type GaAs n-type InP
	Transport in High Magnetic Field	Reliable determination of free carrier concentration & testing of sample homogeneity	n-type GaAs n-type InP
MICROSCALE	Scanning IR Absorption	Apparatus completed, theory developed for n-type GaAs & InP	n, p-type Si (model experiments); n-type GaAs; n-type InP
	SEM-Electron Beam-Induced Current	Instantaneous profiling of diffusion length, lifetime & surface recombination velocity	n, p-type Si (model experiments) n, p-type GaAs



## TRANSPORT IN HIGH MAGNETIC FIELD

Determination of carrier concentration from Hall-effect measurements involves ambiguity related to the value of the Hall factor,  $r$ , which in general can vary between 1.83 and 1, depending on the scattering properties of the semiconductor. However, in high-magnetic fields the Hall factor reduces to  $r = 1$  independent of the nature of the scattering mechanism.

Accordingly, we have carried out Hall-effect measurements in magnetic fields up to 140 k Gauss for GaAs and InP samples. The results showed that for a number of samples the Hall constant vs. magnetic field exhibited anomalous behavior shown in Fig. 1; i.e., the Hall constant exhibited an increase, rather than the expected decrease with increasing magnetic field. Employing our scanning IR absorption technique, we have determined that this anomalous behavior is encountered only with the samples exhibiting carrier concentration inhomogeneities,  $\Delta n/n_{av}$ , exceeding about 20%. This finding, which agrees qualitatively with recent theoretical treatment of electron transport in inhomogeneous semiconductors, shows clearly that Hall measurements as a function of magnetic field provide a reliable means for the assessment of macroscopic homogeneity in InP and GaAs. It should also be noted that according to our findings about 80% of the studied melt-grown GaAs and InP samples (obtained from various suppliers) exhibited inhomogeneities exceeding 20%. Thus, standard, low-magnetic field Hall measurements, commonly used for the characterization of these materials, are totally unreliable.

### SCANNING IR-ABSORPTION

Inhomogeneities in semiconducting materials are commonly recognized as constituting a limiting major factor in microelectronic device applications. Nevertheless, the quantitative determination of inhomogeneities on a micro-scale have been so far possible only in elemental semiconductors (Ge and Si).

The most commonly used method to obtain quantitative carrier distribution profiles is based on spreading resistance measurements. Pressure metal contacts, required for this technique, are highly irreproducible in the case of compound semiconductors, and the technique is not applicable to GaAs or InP characterization.

Accordingly, we have developed a method and constructed an apparatus for the contactless and nondestructive determination of the spatial variation of the free carrier concentration in III-V compounds which is, of course, applicable to other semiconductors. The method is based on the quantitative relationship between infrared absorption and free carrier concentration, and it is applicable to any semiconductor material with free carrier concentration exceeding  $10^{15} \text{ cm}^{-3}$ .

In this method a parallel beam from a  $\text{CO}_2$  laser (tunable between 9.16 and 11.02  $\mu\text{m}$ ) is transmitted through the sample positioned on a stage with x-y motion and a scanning rate ranging from 50 to  $10^{13} \mu\text{m}/\text{min}$ . The light transmitted through the desired area of the sample is focused on a detector (bolometer) through the optics of an IR microscope; the signal from the detector, which is proportional to the intensity of radiation, is amplified and recorded; using a 74X objective the image of an area of about 20  $\mu\text{m}$  in diameter is obtained.

The system permits a continuous monitoring of transmittance of the small wafer area, which is converted, through a data processing system, into variations of carrier concentration and of the compensation ratio. We have recently completed a rigorous theoretical treatment of the pertinent optical phenomena in n-type GaAs and InP required for the quantitative processing of the data. A typical microprofiling of InP obtained recently is given in Fig. 2. It is seen that a two-dimensional quantitative profile of the carrier concentration in InP single crystals has been achieved for the first time. This profile

clearly shows the pronounced inhomogeneities in the presently available melt-grown InP. Similar results have also been obtained with GaAs.

The spatial resolution of our IR-scanning system is about 20  $\mu\text{m}$  and variations in the free carrier density in GaAs as low as  $5 \times 10^{14} \text{ cm}^{-3}$  in n-type and  $2.5 \times 10^{14} \text{ cm}^{-3}$  in p-type material can be detected.

Employing the same experimental system and a theoretical model we have developed we can determine in GaAs and InP the average value of the compensation ratio as well as its variations. It should be noted that this approach can be readily extended to any semiconductor.

#### SEM-ELECTRON BEAM-INDUCED CURRENT

In our approach scanning electron microscopy (SEM) is used primarily in the electron beam-induced current (EBIC) mode. Thus, the electron beam represents in essence a highly focused excitation source for excess minority carriers which are collected by a Schottky barrier or a p-n junction.

We have installed an SEM and accessory electronics especially designed for our EBIC mode approach. In parallel, we have been pursuing a theoretical and experimental study to advance our understanding of the excitation and recombination processes associated with the EBIC mode. In these studies we have used Si as a convenient model material, and we have obtained and confirmed high resolution profiles such as the minority carrier diffusion length, the lifetime, and in certain instances, the dopant profile. For the first time a direct correlation has been achieved on a microscale between compositional inhomogeneities and electronics parameters such as minority carrier diffusion length and lifetime.

We have utilized this technique to analyze diffusion length and the lifetime distribution in melt-grown and epitaxially grown GaAs. The results



provided direct evidence of out-diffusion of defects from substrate to epitaxially grown layers.

Extensive experimental work is in progress devoted to the extension of EBIC-mode technique to temperatures well below and well above room temperatures. In spite of inherent technical difficulties, we consider such an extension of key importance in identifying the specific mechanisms of minority carrier recombination which are the controlling factors in device performance.

TABLE 2

Electron Mobility, Carrier Concentration and Compensation Ratio  
in n-type InP at 300 K

Concentration	Compensation Ratio												
	0	.1	.2	.3	.4	.5	.6	.7	.75	.80	.85	.90	.95
	Electron Mobility ( $\text{cm}^2/\text{Vsec}$ )												
$1.0 \times 10^{15}$	4710	4690	4660	4620	4570	4510	4410	4270	4160	4020	3820	3490	2900
1.5	4670	4630	4590	4540	4480	4390	4270	4090	3970	3800	3560	3210	2610
2	4640	4600	4550	4490	4410	4300	4160	3960	3810	3630	3380	3010	2420
3	4570	4510	4450	4370	4270	4140	3970	3730	3570	3360	3090	2720	2150
4	4520	4450	4370	4280	4160	4010	3820	3560	3380	3170	2900	2530	1980
5	4460	4390	4300	4190	4060	3900	3690	3410	3230	3020	2750	2380	1840
6	4420	4340	4240	4120	3980	3810	3590	3300	3120	2900	2620	2270	1740
7	4380	4290	4180	4060	3910	3730	3500	3200	3010	2790	2520	2170	1650
8	4330	4230	4120	3990	3830	3640	3410	3110	2920	2700	2440	2090	1570
9	4300	4200	4080	3940	3780	3580	3340	3030	2850	2630	2360	2020	1510
$1.0 \times 10^{16}$	4250	4140	4010	3870	3700	3500	3250	2950	2760	2550	2290	1950	1450
1.5	4080	3950	3800	3640	3460	3240	2990	2690	2500	2300	2044	1720	1240
2	3960	3820	3660	3480	3290	3070	2810	2510	2330	2120	1880	1560	1100
3	3770	3610	3440	3250	3050	2820	2570	2270	2100	1900	1660	1360	918
4	3630	3460	3280	3090	2880	2660	2400	2110	1940	1750	1510	1220	800
5	3530	3350	3170	2970	2770	2540	2290	2000	1830	1640	1410	1120	718
6	3440	3270	3080	2880	2670	2440	2190	1900	1740	1550	1320	1040	654
7	3370	3190	3000	2800	2590	2360	2120	1830	1660	1480	1250	973	604
8	3310	3130	2940	2730	2530	2300	2050	1770	1600	1410	1190	920	563
9	3260	3070	2880	2680	2470	2250	2000	1710	1550	1360	1140	875	530
$1.0 \times 10^{17}$	3220	3030	2830	2630	2420	2200	1950	1660	1500	1320	1100	835	501
1.5	3090	2900	2700	2490	2280	2060	1800	1520	1360	1180	970	723	423
2	2960	2760	2560	2350	2140	1910	1660	1370	1210	1040	839	611	345
3	2840	2640	2430	2210	1990	1750	1500	1220	1060	896	712	507	277
4	2770	2560	2340	2120	1890	1650	1400	1120	967	806	633	444	239
5	2720	2500	2270	2050	1820	1570	1320	1040	896	741	577	400	213
6	2680	2450	2220	1990	1760	1510	1260	987	844	694	536	369	194
7	2650	2410	2180	1940	1710	1460	1210	942	802	657	505	346	181
8	2620	2380	2140	1900	1660	1420	1160	900	764	623	477	325	169
9	2590	2350	2110	1860	1630	1380	1130	867	733	596	455	309	160
$1.0 \times 10^{18}$	2570	2320	2080	1830	1590	1350	1100	839	708	573	436	295	152
1.5	2470	2210	1960	1710	1460	1220	979	737	617	495	373	250	128
2	2390	2130	1870	1620	1380	1140	904	674	561	448	336	224	113
3	2290	2010	1750	1500	1260	1030	811	598	495	393	293	194	98
4	2210	1930	1670	1420	1190	965	755	553	456	361	268	177	89
5	2150	1880	1610	1360	1140	920	717	523	431	340	252	166	83
6	2100	1830	1560	1320	1100	886	687	501	411	325	241	158	79
7	2070	1790	1530	1290	1070	861	667	484	398	314	232	152	76
8	2040	1760	1500	1260	1040	838	647	470	386	304	225	148	74
9	2010	1740	1480	1240	1020	821	635	462	378	296	219	144	72
$1.0 \times 10^{19}$	1990	1710	1460	1230	1010	809	624	452	370	289	215	141	71

TABLE 3

Free Carrier Absorption in n-type InP  
at 300 K,  $m^* = 0.078$

Concentration $\text{cm}^{-3}$	Free Carrier Absorption		
	$\alpha_{\text{imp}}$	$\alpha_{\text{ac}}$	$\alpha_{\text{op}}$
$1.0 \times 10^{15}$		0.003	0.058
1.5		0.005	0.087
2	0.001	0.006	0.116
3		0.010	0.174
4	0.001	0.013	0.231
5	0.001	0.016	0.289
6	0.001	0.019	0.346
7	0.002	0.022	0.404
8	0.002	0.025	0.461
9	0.003	0.029	0.518
$1.0 \times 10^{16}$	0.004	0.034	0.623
1.5	0.008	0.052	0.932
2	0.014	0.069	1.239
3	0.031	0.104	1.850
4	0.056	0.139	2.456
5	0.086	0.173	3.051
6	0.123	0.208	3.646
7	0.167	0.243	4.240
8	0.217	0.278	4.815
9	0.273	0.313	5.397
$1.0 \times 10^{17}$	0.314	0.325	5.578
1.5	0.690	0.491	8.227
2	1.201	0.660	10.79
3	2.602	1.005	15.75
4	4.474	1.360	20.52
5	6.790	1.726	25.16
6	9.510	2.100	29.65
7	12.64	2.488	34.11
8	16.13	2.879	38.44
9	20.00	3.285	42.75
$1.0 \times 10^{18}$	24.22	3.699	47.01
1.5	50.28	5.912	67.80
2	83.91	8.354	88.02
3	170.3	13.87	127.0
4	276.7	20.12	164.1
5	396.1	26.98	199.6
6	522.8	34.34	233.4
7	653.3	42.16	266.0
8	784.9	50.22	269.8
9	917.9	58.73	326.7
$1.0 \times 10^{19}$	1052	67.54	355.6



Compensation Ratio

Concentration	0	.1	.2	.3	.4	.5	.6	.7	.75	.8	.85	.9	.95
$1.0 \times 10^{13}$	$3.06 \times 10^5$	$2.98 \times 10^5$	$2.88 \times 10^5$	$2.77 \times 10^5$	$2.63 \times 10^5$	$2.46 \times 10^5$	$2.25 \times 10^5$	$1.99 \times 10^5$	$1.83 \times 10^5$	$1.64 \times 10^5$	$1.42 \times 10^5$	$1.15 \times 10^5$	$8.01 \times 10^4$
1.5	2.91	2.80	2.68	2.54	2.39	2.20	1.98	1.72	1.56	1.39	1.19	$9.58 \times 10^4$	6.64
2	2.77	2.65	2.52	2.37	2.20	2.01	1.79	1.53	1.39	1.23	1.05	8.41	5.78
3	2.56	2.42	2.27	2.11	1.94	1.74	1.53	1.30	1.17	1.03	$8.76 \times 10^4$	6.97	4.72
4	2.38	2.24	2.08	1.92	1.75	1.56	1.36	1.15	1.03	$9.05 \times 10^4$	7.68	6.09	4.05
5	2.25	2.09	1.94	1.77	1.61	1.43	1.24	1.04	0.93	8.19	6.92	5.47	3.58
6	2.13	1.98	1.82	1.66	1.49	1.32	1.15	$9.60 \times 10^4$	8.60	7.54	6.36	5.00	3.22
7	2.03	1.87	1.72	1.56	1.40	1.24	1.07	8.96	8.02	7.02	5.91	4.62	2.94
8	1.92	1.77	1.62	1.47	1.31	1.16	1.00	8.35	7.47	6.52	5.48	4.26	2.68
9	1.87	1.71	1.56	1.41	1.26	1.11	$9.60 \times 10^4$	8.00	7.15	6.23	5.23	4.04	2.51
$1.0 \times 10^{14}$	$1.80 \times 10^5$	$1.65 \times 10^5$	$1.50 \times 10^5$	$1.35 \times 10^5$	$1.21 \times 10^5$	$1.06 \times 10^5$	$9.16 \times 10^4$	$7.62 \times 10^4$	$6.81 \times 10^4$	$5.93 \times 10^4$	$4.96 \times 10^4$	$3.81 \times 10^4$	$2.35 \times 10^4$
1.5	1.55	1.41	1.27	1.14	1.02	$8.91 \times 10^4$	7.65	6.33	5.61	4.87	4.02	3.03	1.80
2	1.38	1.25	1.13	1.01	$8.97 \times 10^4$	7.85	6.72	5.53	4.89	4.20	3.44	2.55	1.48
3	1.17	1.06	$9.49 \times 10^4$	$8.46 \times 10^4$	7.50	6.33	5.55	4.52	3.97	3.27	2.71	1.96	1.10
4	1.04	$9.36 \times 10^4$	8.39	7.47	6.60	5.72	4.84	3.90	3.40	2.86	2.27	1.62	$8.95 \times 10^3$
5	$9.46 \times 10^4$	8.50	7.60	6.75	5.95	5.14	4.32	3.45	2.99	2.50	1.97	1.39	7.58
6	8.76	7.86	7.02	6.22	5.47	4.71	3.93	3.12	2.69	2.34	1.75	1.23	6.62
7	8.21	7.36	6.56	5.80	5.09	4.36	3.63	2.86	2.46	2.03	1.58	1.10	5.91
8	7.74	6.93	6.17	5.44	4.76	4.07	3.37	2.64	2.26	1.86	1.44	1.10	5.33
9	7.36	6.58	5.85	5.15	4.49	3.83	3.16	2.46	2.10	1.72	1.33	$9.20 \times 10^3$	4.88
$1.0 \times 10^{15}$	7.04	6.29	5.58	4.91	4.27	3.63	2.98	2.31	1.97	1.61	1.24	8.53	4.51
1.5	5.87	5.22	4.60	4.01	3.46	2.90	2.35	1.80	1.52	1.23	$9.37 \times 10^3$	6.37	3.33
2	5.16	4.56	4.00	3.47	2.97	2.47	1.98	1.50	1.26	1.01	7.67	5.18	2.70
3	4.27	3.74	3.25	2.79	2.36	1.95	1.54	1.15	$9.58 \times 10^3$	$7.67 \times 10^3$	5.77	3.87	2.00
4	3.72	3.25	2.80	2.39	2.01	1.64	1.29	$9.56 \times 10^3$	7.93	6.32	4.74	3.17	1.63
5	3.33	2.89	2.48	2.11	1.76	1.43	1.12	8.24	6.82	5.42	4.05	2.71	1.39
6	3.05	2.64	2.26	1.90	1.59	1.28	1.00	7.34	6.06	4.81	3.59	2.39	1.23
7	2.82	2.43	2.07	1.74	1.45	1.17	$9.07 \times 10^3$	6.63	5.47	4.34	3.23	2.15	1.10
8	2.63	2.26	1.92	1.61	1.34	1.07	8.34	6.08	5.01	3.97	2.95	1.96	1.01
9	2.48	2.13	1.80	1.51	1.25	1.00	7.76	5.65	4.65	3.68	2.74	1.82	$9.30 \times 10^2$
$1.0 \times 10^{16}$	$2.35 \times 10^4$	$2.01 \times 10^4$	$1.70 \times 10^4$	$1.42 \times 10^4$	$1.17$	$9.39 \times 10^3$	$7.26 \times 10^3$	$5.28 \times 10^3$	$4.34 \times 10^3$	$3.43 \times 10^3$	$2.53 \times 10^3$	$1.70 \times 10^3$	$8.66 \times 10^2$
1.5	1.92	1.63	1.37	1.14	$9.32 \times 10^3$	7.42	5.70	4.12	3.38	2.67	1.98	1.31	6.67
2	1.67	1.41	1.18	$9.73 \times 10^3$	7.95	6.31	4.83	3.48	2.86	2.25	1.67	1.10	5.58
3	1.38	1.15	$9.55 \times 10^3$	7.86	6.39	5.05	3.86	2.77	2.27	1.78	1.32	$8.69 \times 10^2$	4.38
4	1.20	1.00	8.30	6.81	5.52	4.36	3.32	2.38	1.95	1.53	1.13	7.42	3.73
5	1.08	$9.04 \times 10^3$	7.48	6.12	4.96	3.91	2.97	2.13	1.74	1.36	1.00	6.60	3.31
6	1.00	8.34	6.89	5.64	4.56	3.59	2.73	1.95	1.59	1.25	$9.20 \times 10^2$	6.03	3.02
7	$9.36 \times 10^3$	7.79	6.43	5.25	4.24	3.34	2.53	1.81	1.48	1.16	8.53	5.58	2.79
8	8.68	7.22	5.96	4.87	3.94	3.10	2.36	1.69	1.38	1.08	7.99	5.24	2.62
9	8.44	7.02	5.78	4.72	3.81	2.99	2.27	1.62	1.32	1.03	7.59	4.97	2.48
$1.0 \times 10^{17}$	8.08	6.71	5.53	4.51	3.64	2.85	2.16	1.54	1.26	$9.84 \times 10^2$	7.23	4.72	2.35
1.5	6.92	5.73	4.71	3.84	3.09	2.42	1.83	1.30	1.06	8.29	6.08	3.97	1.97
2	6.22	5.15	4.22	3.44	2.76	2.16	1.63	1.16	$9.45 \times 10^2$	7.38	5.40	3.52	1.75
3	5.38	4.45	3.65	2.96	2.38	1.86	1.40	$9.96 \times 10^2$	8.09	6.31	4.62	3.01	1.49
4	4.90	4.04	3.31	2.69	2.16	1.68	1.27	9.99	7.30	5.69	4.16	2.71	1.34
5	4.63	3.82	3.12	2.53	2.03	1.58	1.19	8.43	6.84	5.33	3.90	2.53	1.25
6	4.31	3.55	2.91	2.36	1.89	1.47	1.11	7.86	6.38	4.97	3.63	2.36	1.17
7	4.09	3.38	2.76	2.24	1.79	1.40	1.05	7.46	6.05	4.72	3.45	2.24	1.11
8	3.96	3.27	2.67	2.16	1.73	1.35	1.02	7.20	5.84	4.55	3.33	2.16	1.07
9	3.88	3.19	2.61	2.11	1.69	1.32	$9.91 \times 10^2$	7.01	5.68	4.42	3.23	2.10	1.04
$1.0 \times 10^{18}$	3.74	3.07	2.51	2.04	1.63	1.27	9.57	6.78	5.48	4.28	3.12	2.03	1.01
1.5	3.37	2.79	2.26	1.83	1.47	1.14	8.61	6.12	4.98	3.85	2.81	1.82	$9.00 \times 10^1$
2	3.71	2.61	2.12	1.72	1.38	1.09	8.02	5.79	4.64	3.63	2.64	1.67	8.50
3	2.70	2.37	2.00	1.48	1.34	$9.16 \times 10^2$	7.51	5.33	4.34	3.34	2.36	1.59	7.60

TABLE 4

Electron Mobility, Carrier Concentration and Compensation Ratio  
in n-type InP at 77 K

TABLE 5

Free Carrier Absorption in n-type InP  
at 77 K,  $m^* = 0.082$

Concentration $\text{cm}^{-3}$	Free Carrier Absorption		
	$\alpha_{\text{imp}}$	$\alpha_{\text{ac}}$	$\alpha_{\text{op}}$
$1.0 \times 10^{15}$		0.001	0.033
1.5		0.001	0.049
2		0.001	0.065
3		0.002	0.097
4	0.001	0.002	0.130
5	0.001	0.003	0.162
6	0.001	0.003	0.194
7	0.002	0.004	0.225
8	0.002	0.004	0.257
9	0.003	0.005	0.289
$1.0 \times 10^{16}$	0.003	0.005	0.320
1.5	0.007	0.008	0.476
2	0.012	0.011	0.629
3	0.028	0.016	0.928
4	0.048	0.022	1.217
5	0.075	0.028	1.503
6	0.106	0.033	1.780
7	0.143	0.039	2.053
8	0.185	0.045	2.321
9	0.232	0.050	2.588
$1.0 \times 10^{17}$	0.284	0.056	2.849
1.5	0.617	0.086	4.127
2	1.066	0.117	5.366
3	2.296	0.181	7.793
4	3.949	0.250	10.19
5	6.009	0.322	12.60
6	8.460	0.398	15.02
7	11.27	0.476	17.41
8	14.49	0.560	19.90
9	18.05	0.646	22.38
$1.0 \times 10^{18}$	21.96	0.736	24.89
1.5	46.49	1.229	37.69
2	78.85	1.798	50.91
3	165.13	3.147	76.40
4	276.8	4.751	98.46
5	405.0	6.57	118.6
6	533.3	8.527	137.7

FIGURE CAPTIONS

Figure 1. Hall factor as a function of magnetic field.

Figure 2. Scanning IR absorption two-dimensional profile of n-type InP.





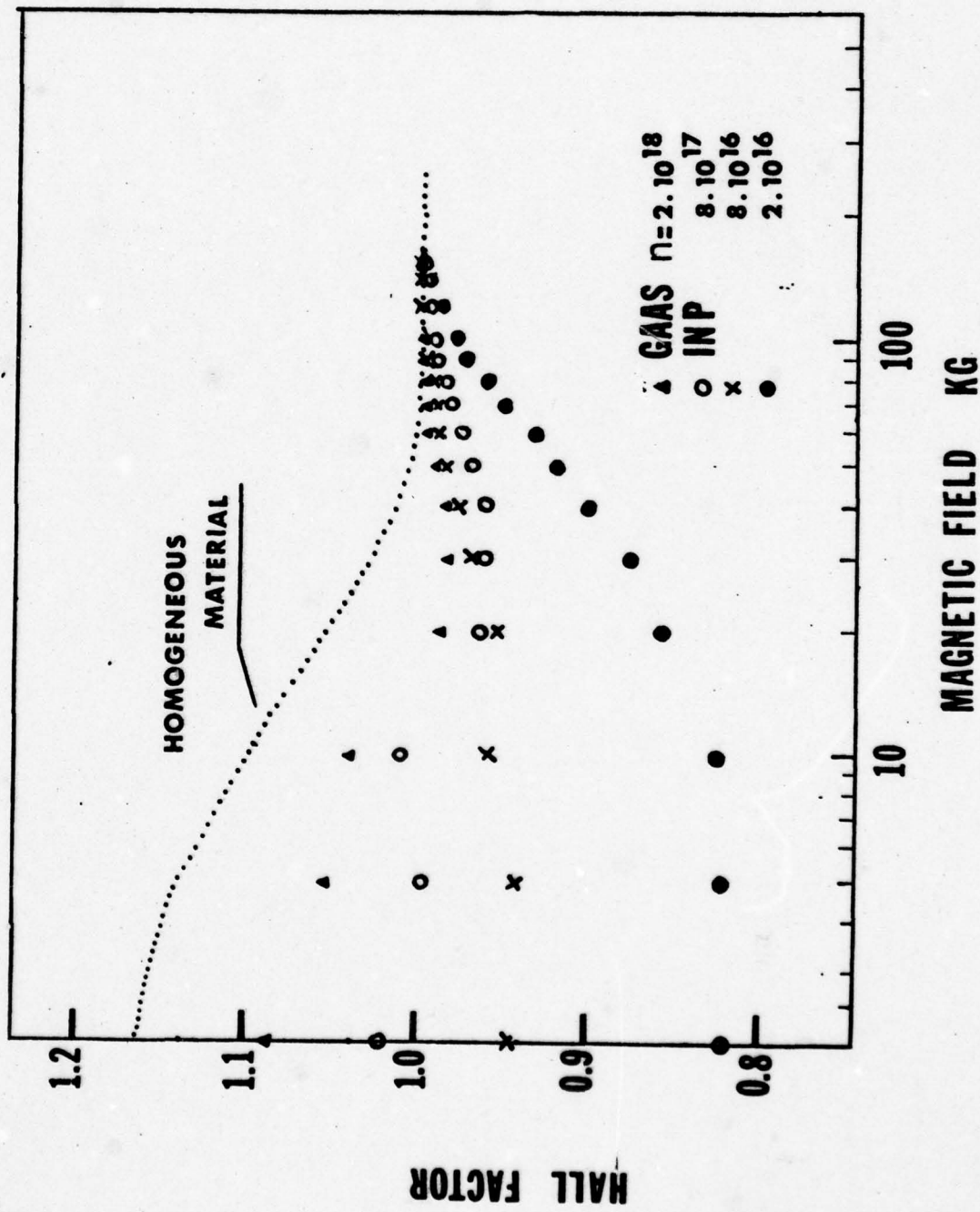


Figure 1

ELECTRON CONCENTRATION  
—  $5 \times 10^{17}$  —

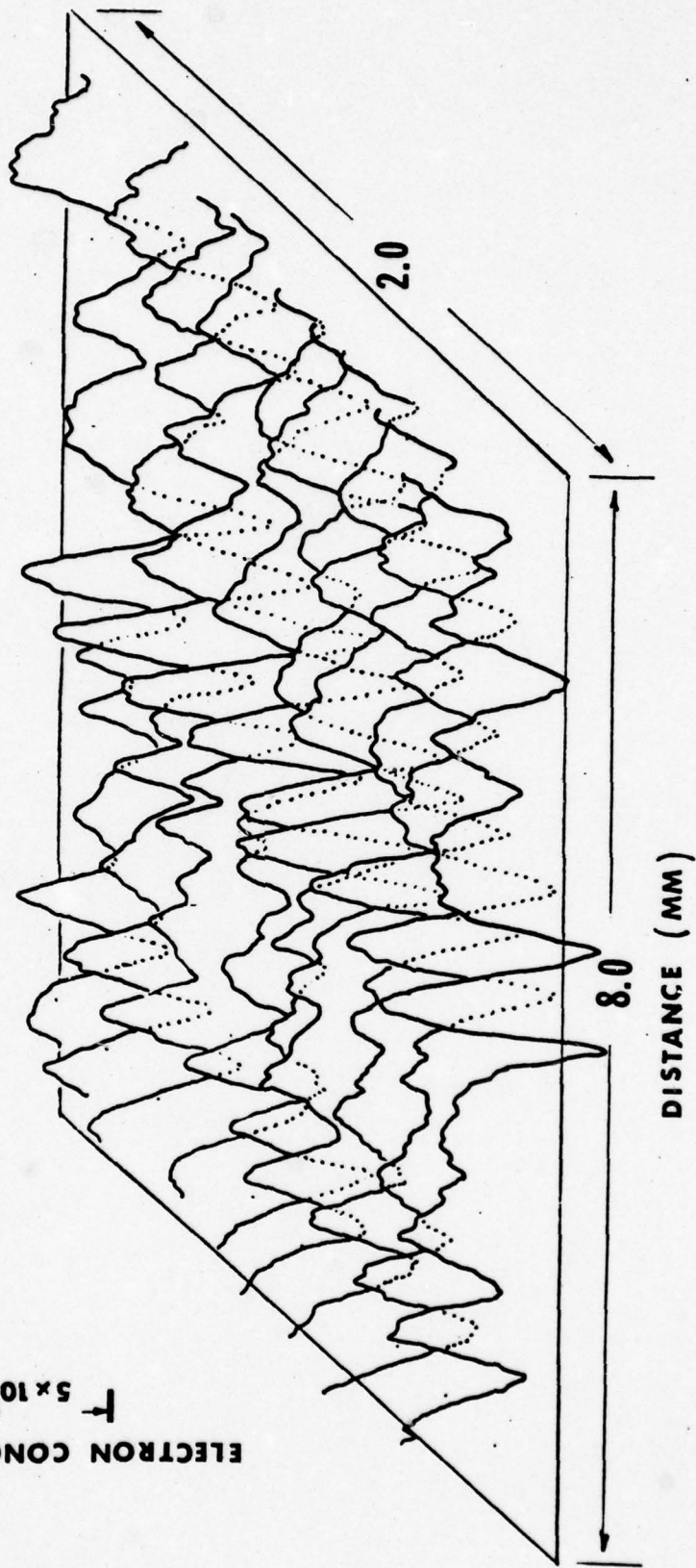


Figure 2

Appendix to Final Report on  
ELECTRONIC CHARACTERISTICS OF  
III-V COMPOUNDS

ELECTRON MOBILITY AND FREE CARRIER ABSORPTION IN GaAs;  
DETERMINATION OF THE COMPENSATION RATIO

W. Walukiewicz,\* J. Lagowski,\* L. Jastrzebski,  
M. Lichtensteiger,\*\* and H. C. Gatos

Department of Materials Science and Engineering  
Massachusetts Institute of Technology  
Cambridge, Massachusetts 02139

ABSTRACT

Theoretical calculations of electron mobility and free carrier absorption in n-type GaAs at room temperature were carried out taking into consideration all major scattering processes. It was found that satisfactory agreement between theoretical and experimental results on free carrier absorption is obtained only when the effect of compensation is quantitatively taken into account. In conjunction with experimental studies it is shown that the electron mobility (for  $n > 10^{15} \text{ cm}^{-3}$ ) and free carrier absorption (for  $n > 10^{16} \text{ cm}^{-3}$ ) are sufficiently sensitive to the ionized impurity concentration to provide a

-----

\*On leave from Institute of Physics, Polish Academy of Sciences, Warsaw, Poland.

\*\*Present address: Coulter Systems Corporation,  
35 Wiggins Avenue, Bedford, Massachusetts 01730.



reliable means for determining the compensation ratio. Convenient procedures are presented for the determination of the compensation ratio from the free-carrier absorption coefficient and from the computed values of room temperature electron mobility. Values of the compensation ratio obtained by these two procedures are in good agreement provided the carrier concentration variations in the material are not appreciably greater than 10%

## I. INTRODUCTION

III-V semiconductors usually exhibit an appreciable degree of compensation. Knowledge of the extent of compensation is important for the understanding of the basic electronic characteristics of these materials and their devices and for the evaluation of crystal growth processes. The methods for determining the compensation are usually related to the fact that the compensation reduces the free carrier concentration

and it enhances free carrier scattering by ionized impurities.

In GaAs, because of the small donor ionization energy ( $\sim 5$  meV), the accurate determination of donor and acceptor concentrations from free carrier concentration changes must be carried out at temperatures well below  $15^{\circ}\text{K}$ . Similarly, the determination of the compensation ratio from the amplitude of Schubnikov de Haas oscillations, as proposed recently,<sup>(1)</sup> must be carried out at  $4.2^{\circ}\text{K}$ . The low temperature requirements render these methods inaccessible for routine needs. Instead, methods based on scattering of free carriers by ionized impurities are employed. The reliable determination of the compensation ratio from free carrier scattering by ionized impurities is complicated, however, by the fact that longitudinal optical phonons contribute significantly to the overall scattering.<sup>(2)</sup> For this polar mode scattering, the relaxation time cannot be defined except for low temperatures.<sup>(3)</sup> Accordingly, it is necessary to use variational<sup>(4)</sup> or iterative

procedures<sup>(2)</sup> to combine all relevant scattering mechanisms. Earlier approaches<sup>(5, 6)</sup> to the determination of the compensation ratio from electron mobility neglected these aspects. More recently, a rigorous semi-empirical procedure has been formulated<sup>(7, 8)</sup> for determining the compensation ratio in n-type GaAs from the Hall constant and resistivity measurements at 77°C. This procedure takes into consideration all major scattering mechanisms but it is applicable only to nondegenerate material. Theoretical calculations of electron mobility (based on an iterative procedure for solving the Boltzmann equation) including compensation as a parameter and considering all major scattering mechanisms have also been reported.<sup>(2, 9)</sup> Although the screening of polar vibrations by free carriers (which is significant at room temperature for  $n > 10^{17} \text{ cm}^{-3}$ ) was not taken into consideration, these results represent the most reliable theoretical values of electron mobility in GaAs thus far.



Free carrier absorption has been used also for the determination of the compensation ratio in n-type GaAs. (10-12)

In this approach (in contrast to that based on the electron mobility) the ionized impurity contribution to free carrier absorption is separable from contributions by other scattering mechanisms. This approach has not as yet been correlated with compensation ratio values obtained by other methods. Furthermore, the values of free carrier absorption available in the literature are not very reliable because the appropriate material parameters were not used in carrying out the computations. (13)

In the present study, the effect of compensation on two independently measured quantities, i.e., on the electron mobility and on the free carrier absorption, is considered. Theoretical computations of mobility are based on a variational method in the form proposed in ref (4) and they include all major scattering processes and screening effects. Computations

of the free carrier absorption coefficient are based on the approach of ref (10). A comparison is made with experimental results and with data available in the literature. (11, 15-18)

A procedure is outlined for the convenient determination of the compensation ratio from measured values of room temperature electron mobility and from the absorption coefficient at a wavelength of about  $10\mu\text{m}$ .

## II. THEORY

### A. General Considerations

The present theoretical calculations are intended to provide the basis for the determination of compensation ratio (or total density of ionized impurities) in n-type GaAs from independent room temperature measurements of the free carrier absorption and the electron mobility.

The electron mobility,  $\mu$ , and the free carrier absorption coefficient,  $\alpha$ , will be defined as:

$$\mu = \frac{\sigma(0)}{ne} ; \quad \alpha(\omega) = \frac{4\pi\sigma(\omega)}{cn_r} \quad (1)$$

where  $\sigma(0)$  and  $\sigma(\omega)$  are the dc and ac conductivity, respectively;  $n$  is the concentration of free electrons;  $c$  is the velocity of light and  $n_r$  is the refractive index at a given irradiation frequency,  $\omega$ .

When the energy band structure, the electron-phonon coupling constants, and the electron concentration are known, the value of  $\sigma$  can be calculated if the total concentration of ionized impurities is also known. For n-type GaAs, the available material parameters are sufficiently accurate for a quantitative calculation of  $\mu$  and  $\alpha(\omega)$ . For a given temperature, such calculations provide two absolute quantities, i.e.,  $\mu$  and  $\alpha/\omega = \text{constant}$ , and one functional dependence  $\alpha(\omega)$ , each of which can be used to determine the concentration of ionized impurities. Accordingly, in cases where ionized impurity scattering is appreciable, experimentally measured electron mobilities, free carrier absorption coefficients and the



frequency dependence of absorption coefficient can serve as the basis for testing the validity of the theoretical calculations and the reliability of the procedure for the determination of the compensation ratio.

In general, dc and ac conductivities can be treated in the same theoretical framework. In practice, however, it has been shown that dc conductivity is satisfactorily obtained from the solution of the semiclassical Boltzmann equation, (2, 4, 19) whereas ac conductivity can be conveniently obtained from second order perturbation theory. (10, 20-22) Both approaches are utilized in the present study; the computations are carried out using the material parameters given in Table (I) and discussed in detail in ref (2).

In view of the high (1.43 eV) and direct energy gap of GaAs, a single spherical, and parabolic conduction band described by an effective mass,  $m^*$ , will be assumed. With such an approximation, the electron mobility is slightly overestimated

and the free carrier absorption is underestimated. For this reason, an effective mass  $m^*/m_0 = 0.068$  is used, which is somewhat higher than the exact value of the effective mass

$$m^*/m_0 = 0.064 \pm 0.002 \text{ at the band edge of GaAs. (23)}$$

In the theoretical approach adopted in the present study, dilute solid solutions are assumed; i.e., interactions between impurities, quantum corrections for ionized impurity scattering<sup>(24)</sup> and differences in the short range part of the impurity potential are not taken into consideration. This assumption sets a limit to the electron (and impurity) concentration, which for n-type GaAs at room temperature can be realistically estimated to be  $3 \times 10^{18} \text{ cm}^{-3}$ . In this respect, it should be pointed out that differences in scattering by various impurities (Te, Se and S) in GaAs at concentrations above  $10^{18} \text{ cm}^{-3}$  have been indicated in refs (25, 16-18). However, a study of the electron mobility in about one thousand GaAs single crystals doped with Te, Se, Sn and Si has failed

to show any consistent differences among the various dopants; (26)  
the only difference (slightly lower mobility) was found in Si  
doped crystals (at concentrations exceeding  $10^{18} \text{ cm}^{-3}$ ); this  
result was apparently due to the amphoteric behavior of Si.

#### B. Free Carrier Absorption

The present analysis will be confined to wavelengths  
greater than  $4\mu\text{m}$ , where transitions between various conduction  
band minima are negligible. Thus, only the lowest conduction  
band with a minimum at the center of the Brillouin zone ( $\Gamma_1$ )  
needs to be considered. The absorption of free carriers in a  
single conduction band constitutes an indirect transition in  
which momentum is conserved through interactions with the  
lattice. Using the approximation of a parabolic conduction  
band, the absorption coefficient can be directly calculated  
from the expressions derived in ref (10).

The total absorption coefficient  $\alpha_t$  is



$$\alpha_t = \alpha_{op} + \alpha_{ac} + \alpha_{imp} \quad (2)$$

where  $\alpha_{op}$ ,  $\alpha_{ac}$  and  $\alpha_{imp}$  are the absorption coefficients corresponding to electron interactions with screened optical phonons, acoustic phonons and screened ionized impurities, respectively. Piezoelectric scattering is not taken into consideration; mobility calculations (see below) showed that for n-type GaAs, at room temperature the contribution of piezoelectric scattering to the total mobility is less than 2%; a similar contribution (which is within the accuracy of the calculations) is expected to the free carrier absorption.

According to ref (10), the absorption coefficients  $\alpha_v$  can be written as follows where  $v$  designates  $op$ ,  $ac$  or  $imp$ :

$$\alpha_v = \frac{C}{z^3} \int_0^{\infty} G_v(x, x'_v) \left\{ f(x) - f(x'_v) \right\} dx \quad (3)$$

where  $f(x) = 1/(e^{x-\eta} + 1)$  is the electron distribution function;  $x = E/k_0T$ ;  $\eta = E_f/k_0T$  and  $z = \hbar\omega/k_0T$  are the reduced electron energy, the Fermi energy and the incident photon energy,

respectively;  $k_0$  is the Boltzmann constant and  $T$  is the absolute temperature. The values of  $C_v$ ,  $G_v$  and  $x'_v$  are:

for optical phonons:

$$C_{op} = 2.96 \times 10^5 (m^*/m_0) \frac{z_\ell}{n_r} \left( \frac{1}{\epsilon_\infty} - \frac{1}{\epsilon_0} \right) \frac{\sinh(z/2)}{\sinh(z_\ell/2) \sinh(z'/2)} \quad (4)$$

$$G_{op} = 2P_{op} \left( 1 + \frac{a^2}{D_{op}} \right) - aL_{op}; \quad x'_{op} = x + z \pm z_\ell$$

for ionized impurities:

$$C_{imp} = 2.175 \times 10^{-5} \frac{N_{imp}}{\epsilon_0 n_r T^2}; \quad G_{imp} = \frac{1}{4} L_{imp} - a \frac{P_{imp}}{D_{imp}} \quad (5)$$

$$x'_{imp} = x + z$$

for acoustic phonons:

$$C_{ac} = 4.79 \times 10^{11} (m^*/m_0)^2 \frac{TE_1^2}{n_r \rho v_\ell^2} \quad (6)$$

$$G_{ac} = P_{ac} B_{ac}$$

$$x'_{ac} = x + z$$

$$\text{where } P_v = (xx'_v)^{1/2}; \quad B_v = x + x'_v \quad (7)$$

$$L_v = \ln \frac{B_v + a + 2P_v}{B_v - a - 2P_v}; \quad D_v = (B_v + a)^2 - 4P_v^2$$

The symbols in equations (4-7) are as follows:

$\epsilon_0, \epsilon_\infty$  are the static and the high frequency dielectric constants

$N_{\text{imp}} = N_D^+ + N_A^-$  is the concentration of ionized impurities

$E_1$  is the conduction band deformation potential

$\rho$  is the crystal density

$v_\ell$  is the longitudinal sound velocity

$z_\ell = \frac{\hbar\omega_\ell}{k_0 T}$  is the reduced energy of longitudinal optical phonons

$m_0$  is the electron mass

$a$  is the reduced screening energy:

$$a = \frac{\hbar^2}{2m^* \ell_D^2 k_0 T} \quad (8)$$

where the screening length  $\ell_D$  is defined as

$$1/\ell_D^2 = 5.80 \times 10^{13} \frac{(m^*/m_0)^{3/2} T^{1/2}}{\epsilon_0} F_{-1/2}(\eta) \quad (9)$$

and  $F_n(\eta)$  is the n-th order Fermi Dirac integral.

It should be noted that  $\alpha_{\text{op}}$  is a sum of two terms given by

eq. (3) which correspond to  $x'_{\text{op}} = x + z - z_\ell$  and  $z' = z - z_\ell$



and to  $x'_{op} = x + z + z_{\ell}$  and  $z' = z + z_{\ell}$ , respectively.

A discussion of the numerical calculations carried out on the basis of equations (2-9) and the GaAs parameters listed in Table (I) will be presented below together with experimental results.

The carrier concentration  $n = N_D^+ - N_A^-$  (where  $N_D^+$  and  $N_A^-$  are the concentrations of ionized donors and acceptors, respectively) enters into equations (2-9) through the reduced Fermi level  $\eta$  according to:

$$n = \frac{2}{\sqrt{\pi}} N_c F_{1/2}(\eta) \quad (10.1)$$

$$\text{or } n = 5.44 \times 10^{15} \left(\frac{T}{T_0}\right)^{3/2} \times F_{1/2}(\eta) \quad (10.2)$$

where  $N_c$  is the effective density of states in the conduction band.

The compensation ratio,  $\theta$ , is defined as  $\theta = N_A^-/N_D^+$ ; accordingly, the total concentration of the ionized impurities is related to the compensation ratio as follows:

$$N_{imp} = n \frac{1 + \theta}{1 - \theta} \quad (11)$$

It is apparent from eqs. (2-9) that for a given frequency of the incident light, and for a given electron concentration, only the term  $\alpha_{imp}$  depends on the compensation ratio (being proportional to  $N_{imp}$ ). Thus, if  $\alpha_{exp}$  is the measured absorption coefficient in a material with a compensation ratio  $\theta$ , and  $\alpha_{op}$ ,  $\alpha_{ac}$  and  $\alpha_{imp}$  are the absorption coefficients computed (from eqs. 3-9) for the same wavelength and the carrier concentration taking  $\theta = 0$  (i.e.,  $N_{imp} = n$ ), the total concentration of ionized impurities can be determined as follows:

$$N_{imp} = n \frac{\alpha_{exp} - (\alpha_{op} + \alpha_{ac})}{\alpha_{imp}} \quad (12a)$$

which according to eq. (11) leads to the following expression for the compensation ratio:

$$\theta = \frac{\alpha_{exp} - (\alpha_{op} + \alpha_{ac})}{\alpha_{exp} + \alpha_{imp} - (\alpha_{op} + \alpha_{ac})} \quad (12b)$$

The values of  $\alpha_{imp}$ ,  $\alpha_{op}$  and  $\alpha_{ac}$  computed as a function of  $n$  for a wavelength of  $10\mu m$  are given in Table (II).

A direct comparison between the experimental values of absorption coefficient and the theoretical dependence of the total free carrier absorption (computed from eqs. 2-7) on electron concentration is not possible, since samples with varying electron concentration can be characterized by a different degree of compensation. To provide a means for such comparison, a reduced experimental absorption coefficient,  $\alpha_{\text{exp}}^*$  will be introduced representing  $\alpha_{\text{exp}}$  for zero compensation.

$$\alpha_{\text{exp}}^* \equiv \alpha_{\text{exp}} - \frac{N_{\text{imp}}}{n} \alpha_{\text{imp}} \quad (13a)$$

which according to eq. (11) becomes

$$\alpha_{\text{exp}}^* = \alpha_{\text{exp}} - \alpha_{\text{imp}} \left( \frac{2\theta}{1-\theta} \right) \quad (13b)$$

The theoretically obtained data in Table (II) can be used for relating  $\alpha_{\text{exp}}^*$  to the compensation ratio as determined by other means (e.g., by electron mobility measurements). This procedure will be discussed below in conjunction with experimental results. At this time, an analytical extension of the above procedure to other wavelengths will be considered without



resorting to additional numerical calculations. In previous treatments (11, 20-22), approximate analytical expressions have been obtained on the frequency dependence of the absorption coefficient assuming a nondegenerate electron gas. They were found to be in fairly good agreement with experiment even in the case of highly doped materials for which the assumption of nondegeneracy is not satisfied. It can be shown, however, that these results are not inconsistent since similar analytical expressions can be obtained from eqs. (2-9).

Thus, in a spectral region, where:

$\hbar\omega$  is much greater than

$\hbar\omega_0$ ,  $E_F$ ,  $k_0T$  and  $ak_0T$

eqs. (3-7) reduce to:

$$\alpha_{op} \approx \frac{4 C_{op}}{z^{2.5}} F_{1/2}(\eta) \quad \text{or} \quad \frac{\alpha_{op}}{n} = \frac{2\pi^{1/2}}{N_c} \left( \frac{k_0T}{nC} \right)^{2.5} \times C_{op} \times \lambda^{2.5} \quad (14.1)$$

$$\alpha_{imp} \approx \frac{C_{imp}}{z^{3.5}} F_{1/2}(\eta) \quad \text{or} \quad \frac{\alpha_{imp}}{n} = \frac{\pi^{1/2}}{2N_c} \left( \frac{k_0T}{nC} \right)^{3.5} \times \lambda^{3.5} \quad (14.2)$$

$$\alpha_{ac} \approx \frac{C_{ac}}{z^{1.5}} F_{1/2}(\eta) \quad \text{or} \quad \frac{\alpha_{ac}}{n} = \frac{\pi^{1/2}}{2N_c} \left( \frac{k_0T}{nC} \right)^{1.5} \times C_{ac} \times \lambda^{1.5} \quad (14.3)$$

These expressions give the same frequency (or wavelength) dependence of the absorption coefficient as the expressions in refs (11, 20-22). For GaAs at room temperature and in the spectral region of 4-10 $\mu$ m inequality  $\hbar\omega \gg \hbar\omega_0$ ,  $E_F$ ,  $k_0T$  and  $ak_0T$  is fairly well satisfied up to an electron concentration of about  $10^{18}$  cm $^{-3}$ . For higher electron concentration eqs. (14.1-14.3) still constitute a reasonable approximation, for shorter wavelengths (e.g., 4-7 $\mu$ m), in agreement with previously reported experimental results. (11, 15)

According to eqs. (14.1-14.3), the procedure for determining the compensation ratio, from eq. (12), and the numerical values in Table (II) for  $\lambda_0 = 10\mu$ m, can be simply extended to other wavelengths  $\lambda$ , by calculating the absorption coefficient according to the approximate relationships:

$$\alpha_{op, \lambda_1} = \alpha_{op, \lambda_0} (\lambda_1/\lambda_0)^{2.5}; \quad (15)$$

$$\alpha_{imp, \lambda_1} = \alpha_{imp, \lambda_0} (\lambda_1/\lambda_0)^{3.5}$$

$$\alpha_{ac, \lambda_1} = \alpha_{ac, \lambda_0} (\lambda_1/\lambda_0)^{1.5}$$

For an electron concentration  $n = 10^{18} \text{ cm}^{-3}$  and for  $8\mu\text{m} \leq \lambda \leq 12\mu\text{m}$  the error in absorption coefficients calculated according to eq. (15) (rather than from more exact numerical calculation based on eqs. (3-7)) does not exceed 9% for  $\alpha_{imp}$  and 4% for  $(\alpha_{op} + \alpha_{ac})$ . These errors decrease rapidly with decreasing electron concentration.

### C. Electron Mobility

The present computations of electron mobility are based on a variational principle method in the form proposed in ref (4, 19). This method allows to combine all scattering mechanisms without invoking the Matthiessen's rule, and it has been successfully applied to the calculation of mobilities in a number of semiconductor compounds. (3, 19, 27-30)

The following scattering mechanisms are considered:  
 screened optical phonon scattering, <sup>(31)</sup> screened ionized  
 impurity scattering, <sup>(19, 32)</sup> acoustic phonon scattering through



the deformation potential<sup>(33)</sup> and piezoelectric interactions.<sup>(34)</sup>

The final expression used (see Appendix I) is:

$$\mu = 308.6 \left[ \left( \frac{1}{\epsilon^\infty} - \frac{1}{\epsilon_0} \right) \left( \frac{m^*}{m_0} \right)^{3/2} T^{1/2} z_\ell F_{1/2}(\eta) \right]^{-1} \times \frac{D_{3/2, 3/2}}{D} \quad (16)$$

where  $D_{3/2, 3/2}$  and  $D$  are the determinants defined in the appendix.

Mobility values as a function of electron concentration obtained in the present study are shown in Fig. (1) together with results reported in ref (2) where an iterative procedure was used for solving the Boltzman equation; screening of polar scattering intentionally is not included in the calculations shown in Fig. (1) since this type of screening was not included in the calculations of ref (2). It is seen that the two methods are in very good agreement; the observed discrepancy at low and high electron concentration is primarily due to the assumption of a parabolic conduction band used in the present study; in ref (2) a nonparabolic conduction band was used with a slightly smaller band edge effective mass (0.066).

The component electron mobilities (i.e., electron mobilities calculated from eq. (16), for each scattering mechanism acting alone) are shown as a function of electron concentration in Fig. (2). It is seen that the maximum contribution to the total mobility from piezoelectric scattering does not exceed 2%, consistent with the assumption made above in the case of free carrier absorption. It is also seen that screening effects become pronounced for electron concentration exceeding  $10^{17} \text{ cm}^{-3}$ .

In Fig. 3 the total electron mobility calculated from eq. (16) is shown together with the electron mobility obtained by summarizing the component mobilities according to Matthiessen's rule (i.e.,  $1/\mu = \sum_i 1/\mu_i$ ). It is seen that for an electron concentration of  $10^{17} \text{ cm}^{-3}$  Mattheissen's rule leads to an error of about 30%. Thus, in determining the compensation ratio one must rely on the results of numerical calculations of mobility as a function of carrier concentration and compensation

ratio. The results obtained in the present study are summarized in Table (II).

### III. COMPARISON WITH EXPERIMENT

#### A. Experimental Procedure and Sample Homogeneity

Hall effect, dc conductivity and infrared absorption measurements were carried out on n-type GaAs samples with electron concentrations ranging from  $6 \times 10^{15}$  to  $2.6 \times 10^{18} \text{ cm}^{-3}$ .

Melt-grown GaAs single crystals, obtained from commercial suppliers, and two epitaxially grown Te-doped layers (intentionally compensated with Ge) were used in this study. In order to obtain consistent and meaningful results, it was found necessary to assess the homogeneity of the samples. The carrier concentration distribution on a macro- and microscale was determined employing a recently reported IR scanning technique.<sup>(35)</sup> In the melt-grown commercial crystals, the spatial variation of the absorption coefficient, at  $\lambda = 10.6 \mu\text{m}$  was found to be of the order of its average value (or  $\Delta n$  of



the order of  $n_{av}$ ). In such samples the measured mobility can be higher<sup>(36)</sup> and the infrared absorption lower than theoretical limits. Accordingly, only samples with carrier concentration inhomogeneities not exceeding approximately 10% are considered in this study. The parameters of these samples are listed in Table (III).

The experimental values of the electron mobility and electron concentration were obtained from Hall-effect and conductivity measurements. In order to avoid ambiguities associated with the value of the Hall factor,  $r$ , the Hall constant was determined as a function of magnetic field up to a value of 100 KG; the saturation value (which corresponds to  $r = 1$ ) was used to determine the electron concentration.

The results obtained are shown in Fig. (4) together with the theoretical dependence of electron mobility on electron concentration for different compensation ratios. The results of ref (18) which will be discussed below in conjunction

with free carrier absorption are also shown. It is seen that all mobility values are well below the theoretical values at zero compensation. From the electron concentration, and the electron mobility, the compensation ratio for each sample was determined directly from Table (II); the values of  $\theta$  are given in Table (III). The normal range of mobility in commercially available high quality GaAs single crystals is indicated in Fig. (4) by the striped area; in the low electron concentration region, the available GaAs is significantly compensated and typically the total concentration of ionized impurities exceeds by an order of magnitude the electron concentration.

The absorption coefficient was determined from the transmittance,  $T$ , (measured with a Fourier spectrometer) using the expression:

$$T = \frac{(1-R)^2 e^{-\alpha d}}{1-R^2 e^{-2\alpha d}} \quad (17)$$

where  $d$  is the thickness of the sample and  $R$  is the

reflectance of GaAs (e.g., for  $\lambda = 10\mu\text{m}$   $R = 0.28$ ), tabulated values of  $R(\lambda)$  are given in ref (37). For sufficiently thin samples ( $ad < 1$ ) the transmittance measured as a function of the thickness of the sample can also be used to determine  $R(\lambda)$ . Measurements carried out in this study showed that for electron concentrations exceeding  $10^{18} \text{ cm}^{-3}$  and for  $\lambda > 10\mu\text{m}$  the reflectance decreases with increasing electron concentration (see also refs 12, 15). However, for lower electron concentrations,  $R$  was found to be essentially independent of  $n$ .

The transmission measurements, intended to provide a basis for determining the absorption coefficient, were carried out on thick samples and with the exception of sample No. 7, the condition  $ad > 1$  was satisfied for wavelengths in the vicinity of  $10\mu\text{m}$ .

The experimental results on the absorption coefficient for  $\lambda = 10\mu\text{m}$  are given in Fig. (5) together with those available in the literature. For comparison, the theoretical values of



the total absorption coefficient  $\alpha_t$  and the absorption components  $\alpha_{op}$ ,  $\alpha_{imp}$  and  $\alpha_{ac}$  are also given in Fig. (V). As it has been discussed above, these absorption coefficients were computed assuming no compensation. Thus, it is understandable that the experimental values of  $\alpha$  are greater than the theoretical ones. Some of the experimental values of ref (11) are smaller than those computed theoretically. Although the reason for this discrepancy is not clear, it should be noted that in the present study absorption coefficients smaller than those obtained theoretically were observed in samples exhibiting significant carrier concentration inhomogeneities.

#### B. Characteristics of Free Carrier Absorption

As pointed out above, a comparison between the experimental and theoretical dependence of free carrier absorption on the electron concentration for samples of different degrees of compensation can be achieved by reducing the experimental absorption coefficient to zero compensation (eq. 13b).

Such a reduction of the experimental results of Fig. (5) was carried out using the values of compensation ratio determined for each sample from electron mobility (Table III), and the computed values of  $\alpha_{imp}$  as given in Table (II). The results of  $\alpha_{exp}^*$  vs. electron concentration are given in Fig. (6) together with the theoretical dependence of  $\alpha_t(n)$ . The obtained agreement is very good, and it is worth emphasizing that no adjustable parameters were used in calculation of the mobility, which provides the basis for determination of  $\theta$ , and of the free carrier absorption coefficient.

The values of the compensation ratio determined from electron mobilities (Table III) have also been used to compare the experimental and theoretical dependence of the absorption coefficient on the wavelength  $\lambda$ . Typical results are given in Fig. (7). It is seen that very good agreement is obtained when the effect of compensation is quantitatively taken into account. It is also seen that for the lower electron

concentration ( $n = 1.1 \times 10^{17} \text{ cm}^{-3}$ ) the compensation affects noticeably both the absolute value of  $\alpha$  and its wavelength dependence (i.e., the slope  $d\ln\alpha/d\ln\lambda$ ). This behavior is not surprising since, with increasing compensation, the dominant role of polar scattering is superseded by ionized impurity scattering. These two scattering modes lead to different wavelength dependences of the absorption coefficient.

### C. Compensation Ratio

The present results have shown that the measured values of electron mobility (Table III) and the experimental characteristics of the free carrier absorption (concentration and wavelength dependences) are satisfactorily explained by theory taking into account compensation.

As discussed above, the value of the compensation ratio can be determined independently from the electron mobility and the electron concentration (utilizing Table II) and from the free



carrier absorption coefficient (utilizing eq. 12b, and the values of absorption components given in Table II). The values of  $\theta$  obtained by these methods are in very good agreement as shown in Table (III). The differences in values of  $\theta$  are within experimental error which is primarily due to inhomogeneity of the material. In the case of intentionally compensated epitaxial layers (4 and 5 in Table III), the values of  $\theta$  determined (0.67 and 0.76, respectively) here are in good agreement with the nominal compensation ratio estimated from the concentration of impurities introduced during the growth (i.e., 0.7 and 0.75, respectively). Thus, it must be concluded that both procedures for determining the compensation ratio lead to reliable and consistent results.

As pointed out above, the upper limit to which the present approach is applicable corresponds to electron (and impurity) concentrations of about  $3 \times 10^{18} \text{ cm}^{-3}$ . The lower concentration limit is determined by the sensitivity of the room

temperature electron mobility and of the free carrier absorption to ionized impurities. These limits are apparent from Table (II) (and/or Figs. 4 and 5). Thus, for a reliable determination of the compensation ratio from electron mobility, the electron concentration should be greater than  $10^{15} \text{ cm}^{-3}$ , and in the case of free carrier absorption, the electron concentration should be greater than  $10^{16} \text{ cm}^{-3}$ . It should also be emphasized that, for the reliable application of the present procedures, GaAs should be reasonably homogeneous. Thus, it is desirable to supplement measurements of mobility and/or free carrier absorption with measurements of the carrier concentration distribution on a microscale. Employing scanning IR absorption<sup>(35)</sup> for this purpose, it also becomes possible (on the basis of the present study) to obtain a compensation ratio profile with a spatial resolution of about  $20 \mu\text{m}$ .

#### SUMMARY

Theoretical and experimental studies of room temperature

electron mobility and free carrier absorption coefficient have been carried out on n-type GaAs. It was shown that for a total concentration of ionized impurities smaller than  $10^{15} \text{ cm}^{-3}$ , the room temperature electron mobility is dominated by polar scattering (with about 10% contribution from acoustic phonon and piezoelectric scattering) and it approaches a value of about  $8000 \text{ cm}^2/\text{Vsec}$ , in agreement with previous experimental and theoretical results. For impurity concentrations exceeding  $10^{15} \text{ cm}^{-3}$ , the mobility becomes sensitive to ionized impurity scattering permitting the determination of the compensation ratio in the material. It was found, however, that the contribution from ionized impurity cannot be analytically separated from other scattering mechanisms since the application of Matthiessen's rule leads to significant errors. Thus, in determining the compensation ratio, one must rely on the results of numerical calculations. The calculated values of electron mobility as a function of compensation ratio given in Table (II)



can be readily used for the determination of the compensation ratio in n-type GaAs with electron concentrations ranging from  $10^{15}$  to  $3 \times 10^{18} \text{ cm}^{-3}$ .

It was also shown that the free carrier absorption coefficient is sensitive to compensation in GaAs for electron concentrations exceeding  $10^{16} \text{ cm}^{-3}$ . An analysis of the present experimental results and those available in the literature showed that the characteristics of free carrier absorption (concentration and wavelength dependences) can be satisfactorily explained only when compensation is quantitatively accounted for.

A procedure for the determination of the compensation ratio from the value of free carrier absorption coefficient for  $\lambda_0 = 10 \mu\text{m}$  (or other wavelengths  $8 \mu\text{m} \leq \lambda \leq 12 \mu\text{m}$ ), and the calculated values of the component absorption coefficients was outlined. For reasonably homogeneous materials, a good agreement was obtained between the values of compensation ratios

obtained from electron mobility and from free carrier absorption. It should be pointed out, that no fitting parameters other than the compensation ratio were used in comparing the experimental and theoretical results.

It was thus concluded that both the room temperature electron mobility and the free carrier absorption coefficient provide a reliable and consistent means for determining the degree of compensation (or the total concentration of ionized impurities) in n-type GaAs. In the form presented here, these methods can be used as practical procedures requiring relatively simple instrumentation. The electron concentration and mobility can be determined by means of standard conductivity and Hall effect measurements, taking the Hall factor  $r$  as unity; the error due to this assumption is estimated to be about 10% for  $n \approx 10^{15} \text{ cm}^{-3}$  and decreases with increasing carrier concentration.

The free carrier absorption method outlined here

requires the determination of the absorption coefficient for one arbitrarily chosen wavelength in the spectral region  $8\mu\text{m} \leq \lambda \leq 12\mu\text{m}$ . Accordingly, relatively simple IR spectrometric instrumentation is required (e.g., a  $\text{CO}_2$  laser and suitable IR detector). For sufficiently thick samples (satisfying the condition  $\alpha d \geq 1$ ) the error associated with minor changes in reflectance due to electron concentration changes can be neglected (for  $n \leq 3 \times 10^{18} \text{ cm}^{-3}$ ) and one can utilize the values of  $R(\lambda)$  given in ref (36). When the electron concentration, the electron mobility and/or the free carrier absorption coefficient are experimentally determined, the compensation ratio and the total number of ionized impurities can be determined from Table (II) and eqs. (11) or (12).



ACKNOWLEDGEMENTS

The authors are grateful to the National Aeronautics and Space Administration and the Department of the Air Force, Electronic Systems Division, for financial support. They would also like to express their appreciation to the technical staff of the Francis Bitter National Magnet Laboratory for the use of their high field facilities.

ACKNOWLEDGMENTS

APPENDIX

Equation (16) describing low field electron mobility has been obtained with the aid of the variational principle method<sup>(4)</sup> adapted to the case of the screened electron-optical phonon interaction.<sup>(27)</sup> The change of the electron distribution function,  $f$ , can be written in the form:

$$\left( \frac{\partial f}{\partial t} \right)_{\text{coll}} = - Ak \cos \phi \frac{\partial f}{\partial x} L(C) \quad (\text{A.1})$$

where  $x = \frac{E}{k_0 T}$ ;  $E$  is the electron energy,  $k \cos \phi$  is the pro-

jection of the electron wave vector on the electric field direction and

$$A = A(x, T, m_0^*) = 4.768 \times 10^{28} \frac{z_l}{x^{3/2}} \frac{(m^*/m_0)^{1/2}}{T^{1/2}} \left( \frac{1}{\epsilon_\infty} - \frac{1}{\epsilon_0} \right) \quad (\text{A.2})$$

Operator  $L(C)$  consists of four terms describing the different scattering mechanisms considered at present

$$L(C) = L_{\text{opt}}(C) + \frac{C(E)}{A} \left[ \frac{1}{\tau_{\text{imp}}} + \frac{1}{\tau_{\text{ac}}} + \frac{1}{\tau_{\text{pel}}} \right] \quad (\text{A.3})$$

The relaxation times,  $\tau$ , for elastic scattering processes are

Appendix, page 2

given by,

screened ionized impurities: (32)

$$\frac{1}{\tau_{\text{imp}}} = 2.415 \frac{N_{\text{imp}}}{\epsilon_0} \left(\frac{m^*}{m_0}\right)^{-1/2} (xT)^{-3/2} \left[ \ln \left(1 + \frac{4x}{a}\right) - \frac{\frac{4x}{a}}{1 + \frac{4x}{a}} \right] \quad (\text{A.4})$$

acoustic phonon scattering through deformation

potential: (33)

$$\frac{1}{\tau_{\text{ac}}} = 4.167 \times 10^{19} \frac{E_1^2}{\rho v_\ell^2} \left(\frac{m^*}{m_0} T\right)^{3/2} x^{1/2} \quad (\text{A.5})$$

piezoelectric (acoustic mode) scattering: (34)

$$\frac{1}{\tau_{\text{pel}}} = 1.052 \times 10^7 \times h_{14}^2 \left(\frac{3}{C_\ell} + \frac{4}{C_t}\right) \left(\frac{T m^*}{x m_0}\right)^{1/2} \quad (\text{A.6})$$

For screened optical phonon (polar) scattering: (27)

$$\begin{aligned} L_{\text{opt}}(C) = & \frac{f_+}{f} (N+1) C_+ \left[ (R_+ + a) S_+ - a R_+ T_+ - 4U_+ \right] \\ & - 2x \frac{f_+}{f} (N+1) C_+ \left[ S_+ - a T_+ \right] + h(x - z_\ell) \left\{ \frac{N f_-}{f} C_- \right. \\ & \left. \left[ (R_- + a) S_- - a R_- T_- - 4U_- \right] - 2x N C_- \frac{t_-}{f} \left[ S_- - a T_- \right] \right\} \quad (\text{A.7}) \end{aligned}$$

where  $f_\pm = f_0(x \pm z_\ell)$ ;  $C_\pm = C(E \pm \hbar\omega_\ell)$

$$R_\pm = 2x + a \pm z_\ell; U_\pm = \sqrt{x(x \pm z_\ell)}$$



Appendix, page 3

$$T_{\pm} = \frac{4U_{\pm}}{R_{\pm}^2 - 4U_{\pm}^2} ; S_{\pm} = \ln \left[ \frac{R_{\pm} + 2U_{\pm}}{R_{\pm} - 2U_{\pm}} \right]$$

and  $N = \frac{1}{e^{z_{\ell}} - 1}$  is the optical phonon occupation number.

Following the procedure developed in ref (4), one obtains the following expression for electron mobility:

$$\mu = 308.6 \left[ \left( \frac{1}{\epsilon_{\infty}} - \frac{1}{\epsilon_0} \right) \left( \frac{m^*}{m_0} \right)^{3/2} T^{1/2} z_{\ell} F_{1/2}(n) \right]^{-1} \frac{D_{3/2, 3/2}}{D} \quad (\text{A.})$$

where the determinants have forms

$$D_{3/2, 3/2} = \begin{vmatrix} 0 & \beta_0^{(3/2)} & \beta_1^{(3/2)} & \dots \\ \beta_0^{(3/2)} & d_{00} & d_{01} & \dots \\ \beta_1^{(3/2)} & d_{10} & d_{11} & \dots \\ \cdot & \cdot & \cdot & \\ \cdot & \cdot & \cdot & \\ \cdot & \cdot & \cdot & \end{vmatrix} \quad (\text{A.9})$$

$$D = \begin{vmatrix} d_{00} & d_{01} & \dots \\ d_{10} & d_{11} & \dots \\ \cdot & \cdot & \\ \cdot & \cdot & \\ \cdot & \cdot & \end{vmatrix} \quad (\text{A.10})$$

Appendix, page 4

The elements of the determinants are given by the integrals:

$$\beta_r^{(3/2)} = \int_0^{\infty} E^{3/2} \phi_r \frac{\partial f_0}{\partial E} dE \quad (\text{A.11})$$

$$d_{r,s} = \int_0^{\infty} \phi_r L(\phi_s) \frac{\partial f_0}{\partial E} dE \quad (\text{A.12})$$

The functions  $\phi_r$  should represent a complete set of functions of electron energy  $E$ . In the present computations, the set  $\phi_{r(s)} = E^{r(s)}$  was chosen with values of  $r$  and  $s$  equal to 0, 1 and 2, which at room temperature assure an accuracy of the mobility calculations within a few percent. (4, 38)

TABLE I

GaAs parameters used in present computations (300° K)  
(after refs 2 and 9)

low frequency	
dielectric constant, $\epsilon_0$	12.91
high frequency	
dielectric constant, $\epsilon_\infty$	10.91
optical phonon	
energy, $\hbar\omega_0$	36 meV
deformation	
potential, $E_1$	7 eV
longitudinal	
elastic constant, $C_\ell = \rho v_\ell^2$	$14.03 \times 10^{11}$ dyne/cm <sup>2</sup>
piezoelectric	
coefficient, $h_{14}^2 \left( \frac{3}{C_\ell} + \frac{4}{C_t} \right)$	$2.39 \times 10^{-2}$
effective mass, $m^*/m_0$	0.068 (see text)



TABLE II

Computed Values of Electron Mobility and IR Absorption in n-type GaAs

COMPENSATION RATIO	ELECTRON MOBILITY ( $\text{cm}^2/\text{Vsec}$ )										ABSORPTION at $10\mu\text{m}$ ( $\text{cm}^{-1}$ )		
	.0	.1	.2	.3	.4	.5	.6	.7	.8	.9	$\alpha_{\text{imp}}$	$\alpha_{\text{ac}}$	$\alpha_{\text{op}}$
$1 \times 10^{15}$	7810	7760	7700	7620	7530	7400	7220	6940	6490	5590			
1.5	7740	7680	7590	7490	7360	7200	6970	6640	6120	5150			
2	7600	7510	7410	7290	7140	6950	6690	6330	5770	4780			
3	7540	7430	7300	7150	6960	6730	6420	6000	5400	4370			
4	7450	7320	7170	6990	6780	6510	6180	5730	5100	4070			
5	7370	7230	7060	6870	6640	6350	6000	5540	4850	3870			
6	7280	7130	6950	6730	6490	6190	5820	5340	4700	3670			
7	7230	7060	6860	6640	6380	6060	5680	5200	4540	3510			
8	7150	6970	6760	6530	6260	5930	5540	5050	4390	3370			
9	7050	6860	6650	6400	6120	5790	5390	4900	4250	3232			
$1 \times 10^{16}$	6980	6790	6560	6310	6020	5680	5280	4790	4140	3120	.0036	.025	.341
1.5	6710	6480	6230	5950	5640	5280	4870	4370	3720	2710	.0080	.038	.510
2	6500	6250	5980	5680	5360	5000	4580	4080	3430	2440	.0142	.050	.679
3	6190	5920	5630	5320	4980	4610	4180	3680	3030	2060	.032	.075	1.01
4	5970	5690	5380	5060	4720	4340	3910	3410	2760	1820	.056	.100	1.35
5	5810	5510	5200	4870	4520	4140	3710	3200	2560	1640	.087	.126	1.68
6	5680	5370	5050	4720	4370	3980	3550	3040	2400	1510	.125	.152	2.00
7	5570	5260	4940	4600	4250	3860	3420	2910	2270	1400	.169	.178	2.32
8	5480	5160	4840	4490	4140	3740	3300	2790	2160	1320	.220	.203	2.65
9	5400	5080	4750	4400	4040	3640	3200	2690	2060	1240	.277	.229	2.97
$1 \times 10^{17}$	5330	5010	4670	4320	3960	3560	3120	2600	1980	1180	.340	.255	3.28
1.5	5090	4750	4400	4030	3650	3240	2790	2280	1690	960	.746	.387	4.84
2	4910	4540	4160	3780	3390	2970	2520	2030	1470	820	1.29	.521	6.35
3	4730	4350	3960	3560	3160	2730	2280	1790	1270	680	2.79	.796	9.26
4	4530	4130	3730	3320	2920	2490	2050	1590	1100	580	4.82	1.08	12.1
5	4470	4060	3640	3220	2800	2380	1940	1490	1020	530	7.26	1.34	14.8
6	4370	3950	3520	3100	2680	2260	1830	1390	950	480	10.2	1.68	17.5
7	4290	3860	3420	3000	2580	2160	1740	1320	890	450	13.5	1.99	20.1
8	4220	3780	3340	2910	2500	2080	1670	1260	840	420	17.2	2.32	22.7
9	4160	3710	3270	2840	2430	2010	1610	1200	800	400	21.3	2.65	25.3
$1 \times 10^{18}$	4100	3640	3200	2770	2360	1950	1550	1160	770	380	25.8	3.00	27.9
1.5	3860	3400	2950	2520	2130	1740	1370	1010	660	330	53.4	4.85	40.5
2	3690	3220	2780	2360	1980	1600	1250	920	600	290	88.8	6.91	52.8
3	3460	3000	2560	2160	1790	1440	1120	810	530	260	178	11.6	76.6
4	3300	2840	2410	2020	1670	1340	1040	750	480	230	284	16.9	98.6
5	3200	2750	2330	1950	1600	1280	990	710	460	220	400	22.8	120

TABLE III

Compensation Ratios Derived from Mobility and IR Absorption Measurements

SAMPLE NO.	ELECTRON CONCENTRATION ( $\text{cm}^{-3}$ )	GROWTH	DOPANT	HOMOGENEITY $\Delta n/n_{av}$	MOBILITY $\text{cm}^2/\text{Vsec}$	COMPENSATION RATIO, $\theta$ MOBILITY	ABSORPTION
1.	$3 \times 10^{16}$	melt	Te	$\leq 10\%$	2700	$0.83 \pm 0.03$	$0.89 \pm 0.05$
2.	$1.1 \times 10^{17}$	melt	?	$\leq 10\%$	1800	$0.83 \pm 0.03$	$0.85 \pm 0.03$
3.	$5.5 \times 10^{17}$	melt	Te	$\leq 10\%$	3300	$0.25 \pm 0.06$	$0.23 \pm 0.08$
4.*	$8.5 \times 10^{17}$	LPE	Te	$\leq 3\%$	1350	$0.67 \pm 0.03$	$0.65 \pm 0.04$
5.*	$1.5 \times 10^{18}$	LPE	Te	$\leq 3\%$	800	$0.76 \pm 0.02$	$0.77 \pm 0.03$
6.	$2.0 \times 10^{18}$	melt	?	$\leq 15\%$	2100	$0.37 \pm 0.08$	$0.29 \pm 0.08$
7.	$6 \times 10^{15}$	melt	--	$\leq 20\%$	3300	$> .9$	$> .9$
8.	$2.6 \times 10^{18}$	melt	--	$\leq 20\%$	1650	$0.40 \pm 0.1$	$0.3 \pm 0.1$
Ref (18)	$6 \times 10^{17}$	----	Te	----	3600	0.18	0.18
- " -	$1.15 \times 10^{18}$	----	S	----	2600	0.31	0.25
- " -	$1.2 \times 10^{18}$	----	Te	----	3100	0.22	0.22

\*Intentionally compensated with Ge (see text).

REFERENCES

- (1) A. Raymond, J. L. Robert and B. Pistoulet, Proc. VI Int. Symp. on GaAs and Related Compounds, Edinburgh, Sept. 1976, ed. C. Hilsum, The Inst. of Phys., London, p. 105.
- (2) For a recent review see D. L. Rode in "Semiconductors and Semimetals," ed. R. K. Willardson and A. C. Beer, Academic Press, N.Y., 1975, vol. 10, ch. 1.
- (3) H. Ehrenreich, J. Appl. Phys. 32, 2155 (1961).
- (4) D. Howarth and E. H. Sonheimer, Proc. Phys. Soc. A 219, 53 (1953).
- (5) F. J. Reid, in "Compound Semiconductors," vol. I. Preparation of III-V Compounds, Eds. R. K. Willardson and H. L. Goering, Reinhold Publishing Corp., New York, 1962, p. 158.
- (6) H. Kressel and H. Nelson, J. Appl. Phys. 40, 3720 (1969).
- (7) C. M. Wolfe, G. E. Stillman and J. O. Dimmock, J. Appl. Phys. 11, 504 (1970).



- (8) G. E. Stillman and C. M. Wolfe, *Thin Solid Films* 31, 69 (1976); D. L. Rode, *Phys. Rev. B*, 2, 1012 (1970).
- (9) D. L. Rode and S. Knight, *Phys. Rev. B*, 3, 2534 (1971).
- (10) E. Haga and H. Kimura, *J. Phys. Soc. Japan*, 19, 658 (1964).
- (11) K. Osamura and Y. Murakami, *Jap. J. Appl. Phys.* 11, 365 (1972).
- (12) J. K. Kung, W. G. Spitzer, *J. Electrochem. Soc.* 121, 1482, (1974).
- (13) Compare the values of GaAs parameters used in ref (10, 11) with those of Table (I) of ref (2). For a recent discussion of GaAs parameters, see ref (14).
- (14) G. E. Stillman, C. M. Wolfe and J. O. Dimmock, in "Semiconductors and Semimetals," ed. R. K. Willardson and A. C. Beer, Academic Press, N.Y. 1977, vol. 12, ch. 4.
- (15) W. G. Spitzer and J. M. Whelan, *Phys. Rev.* 114, 59 (1959).
- (16) M. G. Milvidskii, V. B. Osvenskii, E. P. Rashevskaya and T. G. Yugova *Soviet Physics, Solid State*, 7, 2784 (1966).

## References, page 3

- (17) E. P. Rashevskaya and V. I. Fistul, Soviet Physics, Solid State 9, 1443 (1967).
- (18) E. P. Rashevskaya and V. I. Fistul, Soviet Physics, Solid State 9, 2849 (1968)
- (19) H. Ehrenreich, Phys. Rev. 120, 1951 (1960).
- (20) H. Y. Fan, W. Spitzer and R. J. Collins, Phys. Rev. 101, 566 (1956).
- (21) R. Rosenberg and M. Lax, Phys. Rev. 112, 843 (1958).
- (22) S. Visvanathan, Phys. Rev. 120, 376 (1960).
- (23) For a recent discussion of GaAs effective mass, see ref (14) p. 180-186.
- (24) E. J. Moore, Phys. Rev. 160, 607 (1967); 160, 618 (1967).
- (25) V. I. Fistul, E. M. Omelyanovskii, O. V. Pelevin and V. B. Ufimtsev, Izv. Akad. Nauk SSSR, ser. Neorganicheskie Materialy, 2, 657 (1966) (in Russian).
- (26) S. M. Sze and J. C. Irvin, Sol. Stat. Elect. 11, 599 (1968).

- (27) H. Ehrenreich, J. Phys. Chem. Solids 2, 131 (1957);  
9, 129 (1959).
- (28) S. L. Lehochky, J. G. Broerman, D. A. Nelson and C. R. Whitsett, Phys. Rev. B, 9, 1598 (1974).
- (29) W. Walukiewicz, J. Phys. C: Solid State Phys. 9, 1945 (1976).
- (30) S. S. Devlin, in "Physics and Chemistry of II-VI Compounds," eds. M. Aven and J. S. Prener, North-Holland Publishing Co., Amsterdam, 1967, ch. 11.
- (31) H. Ehrenreich, J. Phys. Chem. Solids 8, 130 (1959).
- (32) R. B. Dingle, Phil. Mag. 46, 831 (1955).
- (33) W. Shockley, "Electrons and Holes in Semiconductors," Van-Nostrand-Reinhold, Princeton, N.J., 1950.
- (34) J. D. Zook, Phys. Rev. 136, 869 (1964).
- (35) L. Jastrzebski, J. Lagowski and H. C. Gatos, Electrochemical Society Meeting, Seattle, 1978, extended abstracts, vol. 78-1, p. 551; submitted to J. Electrochem. Soc.



## References, page 5

(36) C. M. Wolfe and G. E. Stillman, in "Semiconductors and Semimetals," ed. R. K. Willardson and A. C. Beer, Academic Press, N.Y., 1975, vol. 10, ch. 3.

(37) B. O. Seraphin and H. E. Bennett, in "Semiconductors and Semimetals," eds. R. K. Willardson and A. C. Beer, Academic Press, N.Y., 1967, vol. 3, ch. 12.

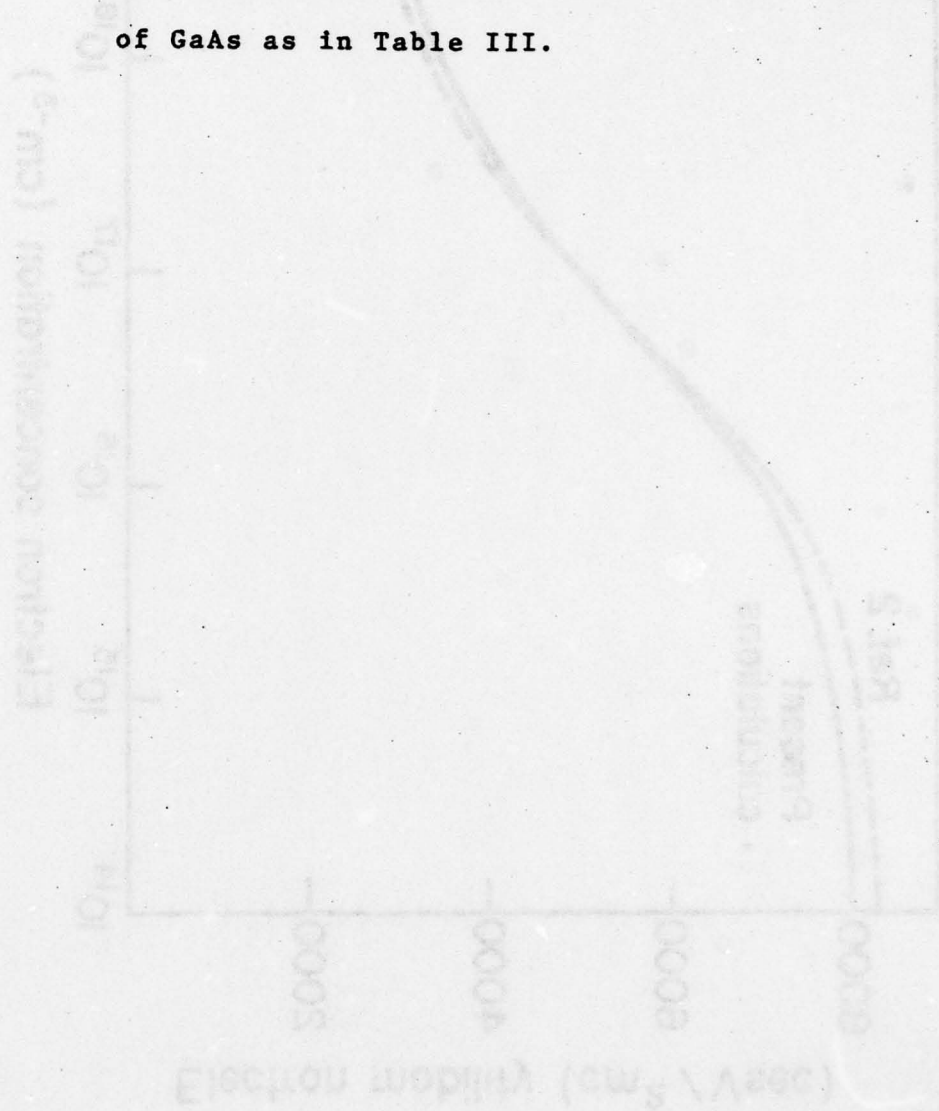
(38) The accuracy of the variational principle method increases with decreasing  $z_l = \frac{\hbar\omega_0}{kT}$ . For GaAs at room temperature  $z_l \approx 1.4$ . A comparison of results in ref (4) and recent calculations in ref (39) shows that the accuracy of variational calculations in the form presented here can be expected to be better than 5%.

(39) C. Hammer and B. Magnusson, Phys. Scripta 6, 206 (1972).

FIGURE CAPTIONS

- Figure 1. Comparison of electron mobilities calculated by a variational method (present calculations) and by an iterative procedure (ref. 2) for n-type GaAs at room temperature; screening of polar scattering is not included (see text).
- Figure 2. Calculated component and total electron mobility as a function of electron concentration in n-type GaAs at room temperature.
- Figure 3. Comparison of electron mobilities in n-type GaAs calculated by a variational method and by Matthiessen's rule employing the component mobilities.
- Figure 4. Theoretical (solid lines) and experimental values of mobility as a function of electron concentration in n-type GaAs for various compensation ratios; the mobility range for commercially available GaAs is also indicated.
- Figure 5. Theoretical and experimental values of absorption coefficient as a function of electron concentration in GaAs at room temperature.
- Figure 6. Theoretical (solid line) and experimental values of absorption coefficient reduced to zero compensation (see text) as a function of electron concentration in GaAs at room temperature; wavelength of radiation  $\lambda = 10 \mu\text{m}$ .
- Figure 7. Absorption coefficient as a function of wavelength.

Solid and dotted lines correspond to theoretical values, neglecting compensation, and dotted lines correspond to theoretical values obtained by taking into account compensation as determined from electron mobility; ●, ■ and ▲ are experimental values obtained with samples 6, 3 and 2, respectively, of GaAs as in Table III.





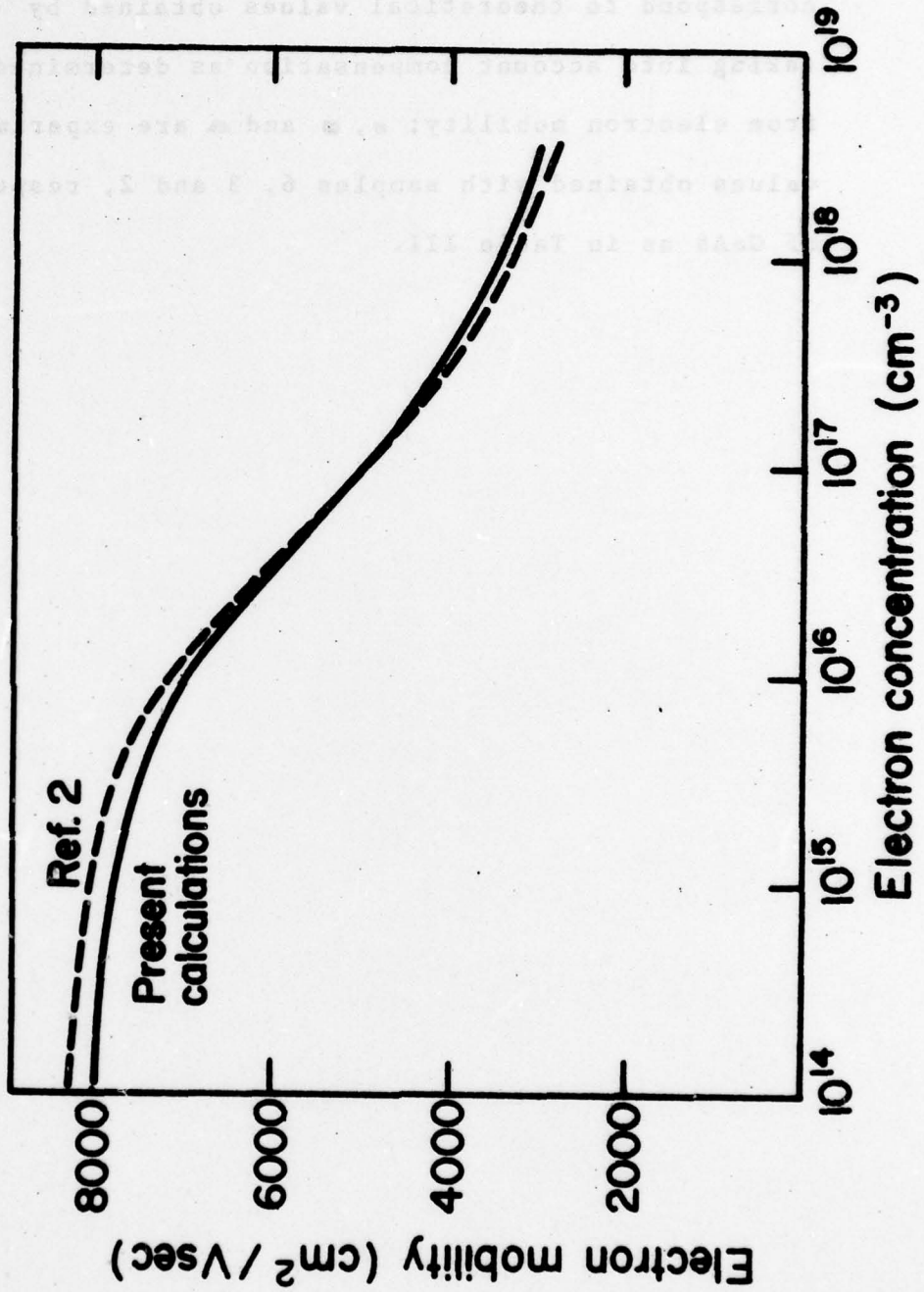


Figure 1

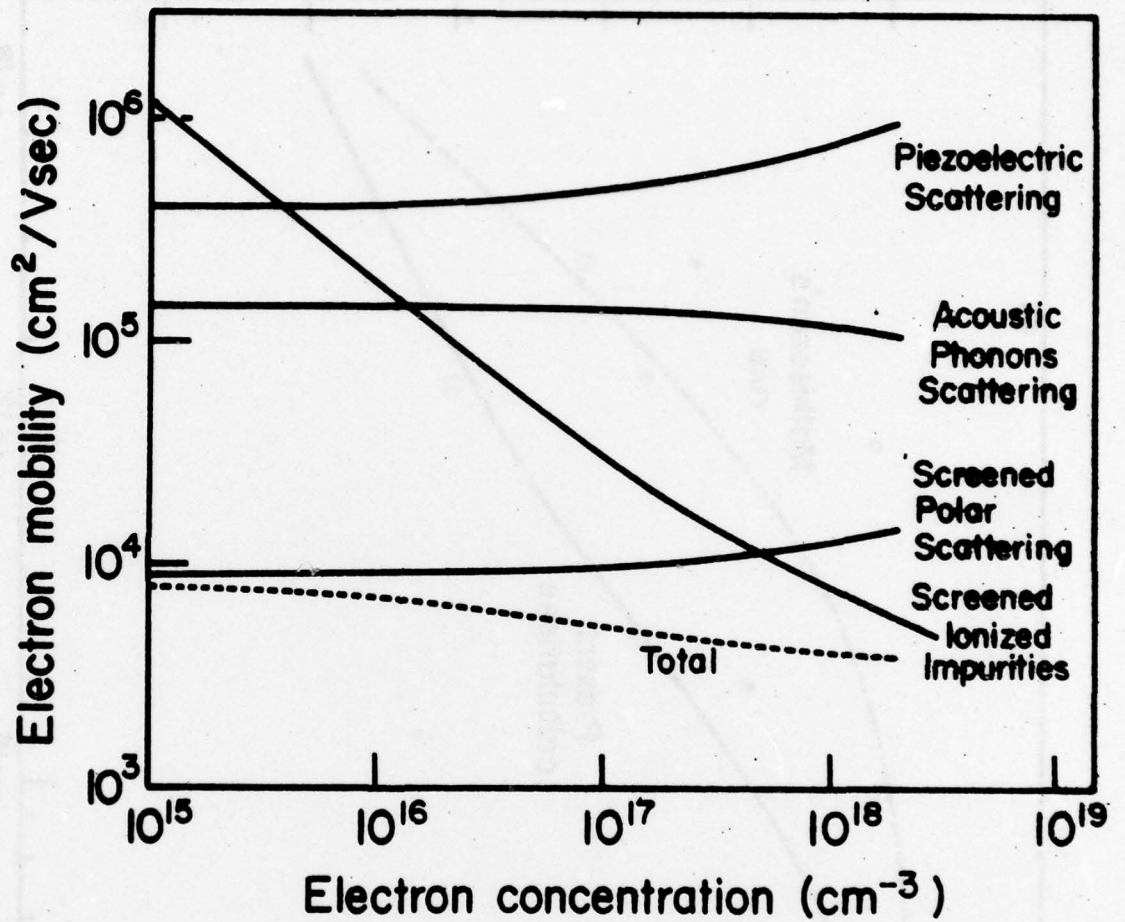


Figure 2

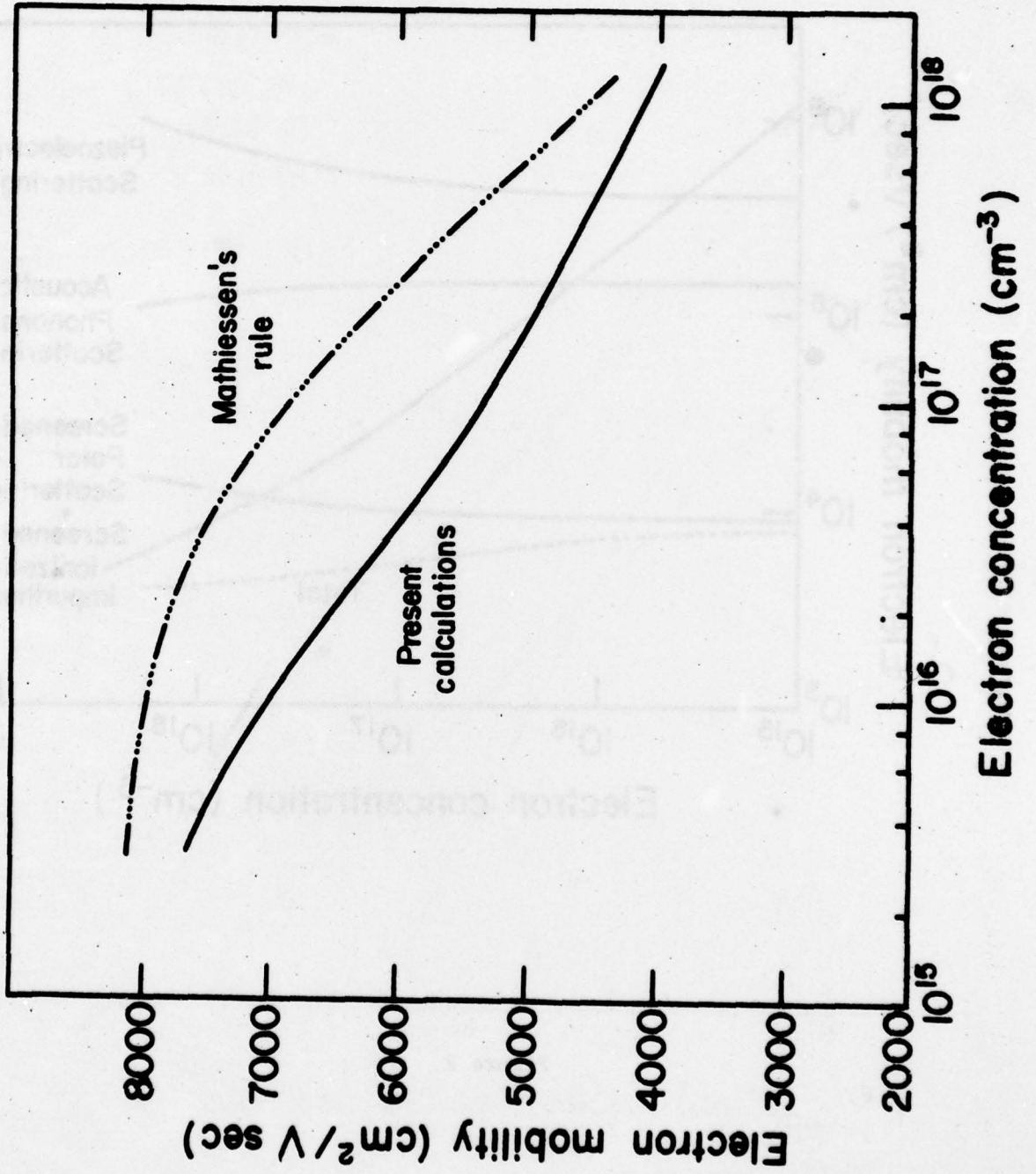


Figure 3



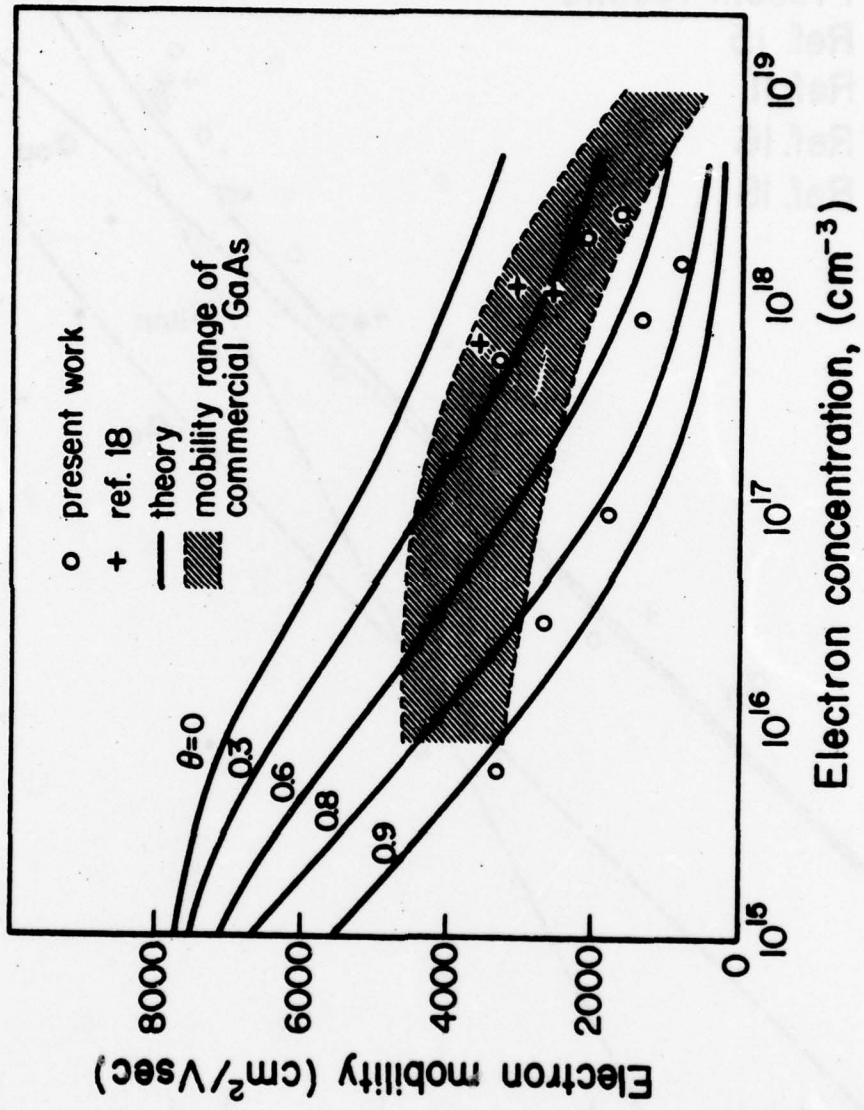


Figure 4

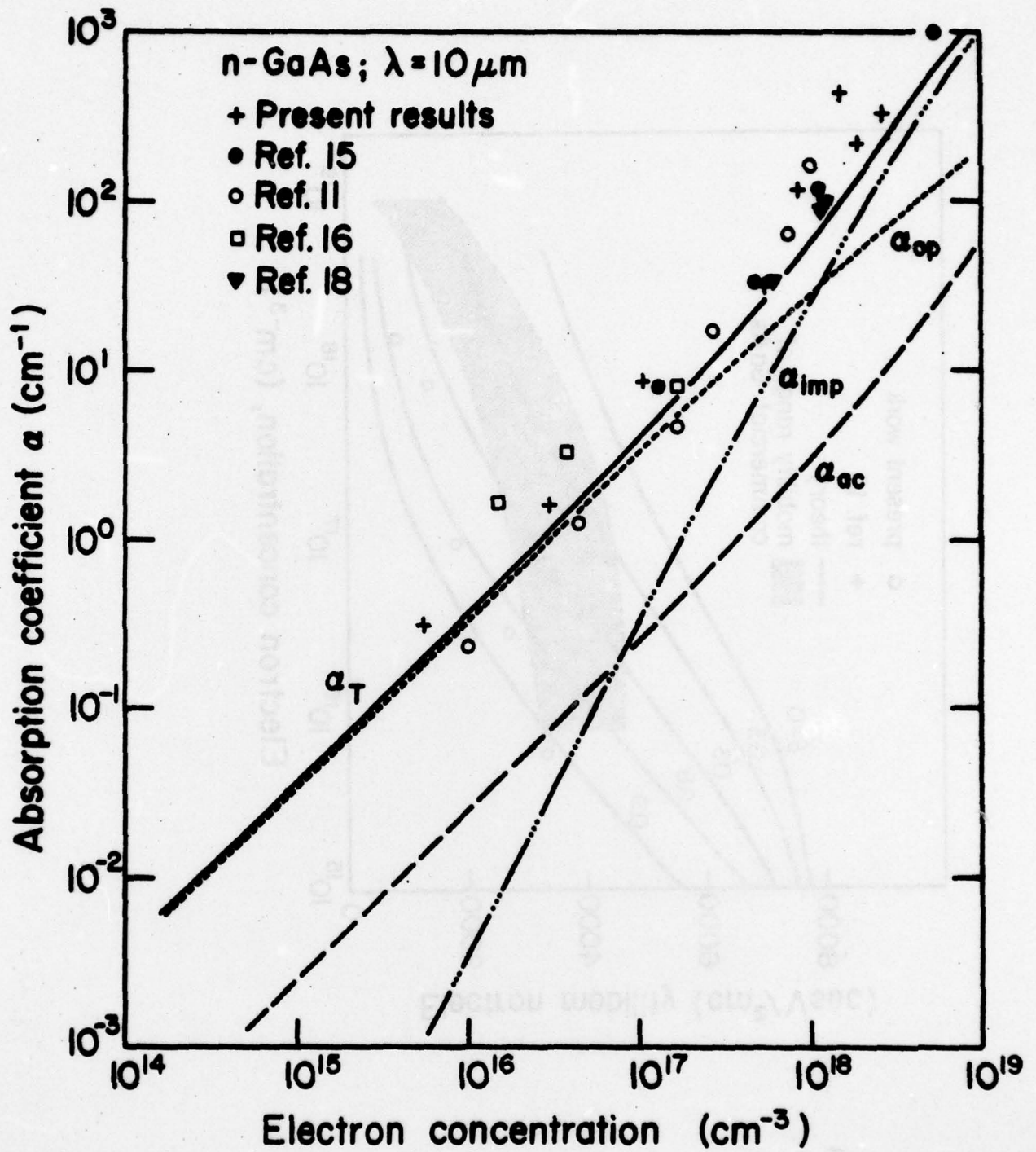


Figure 5

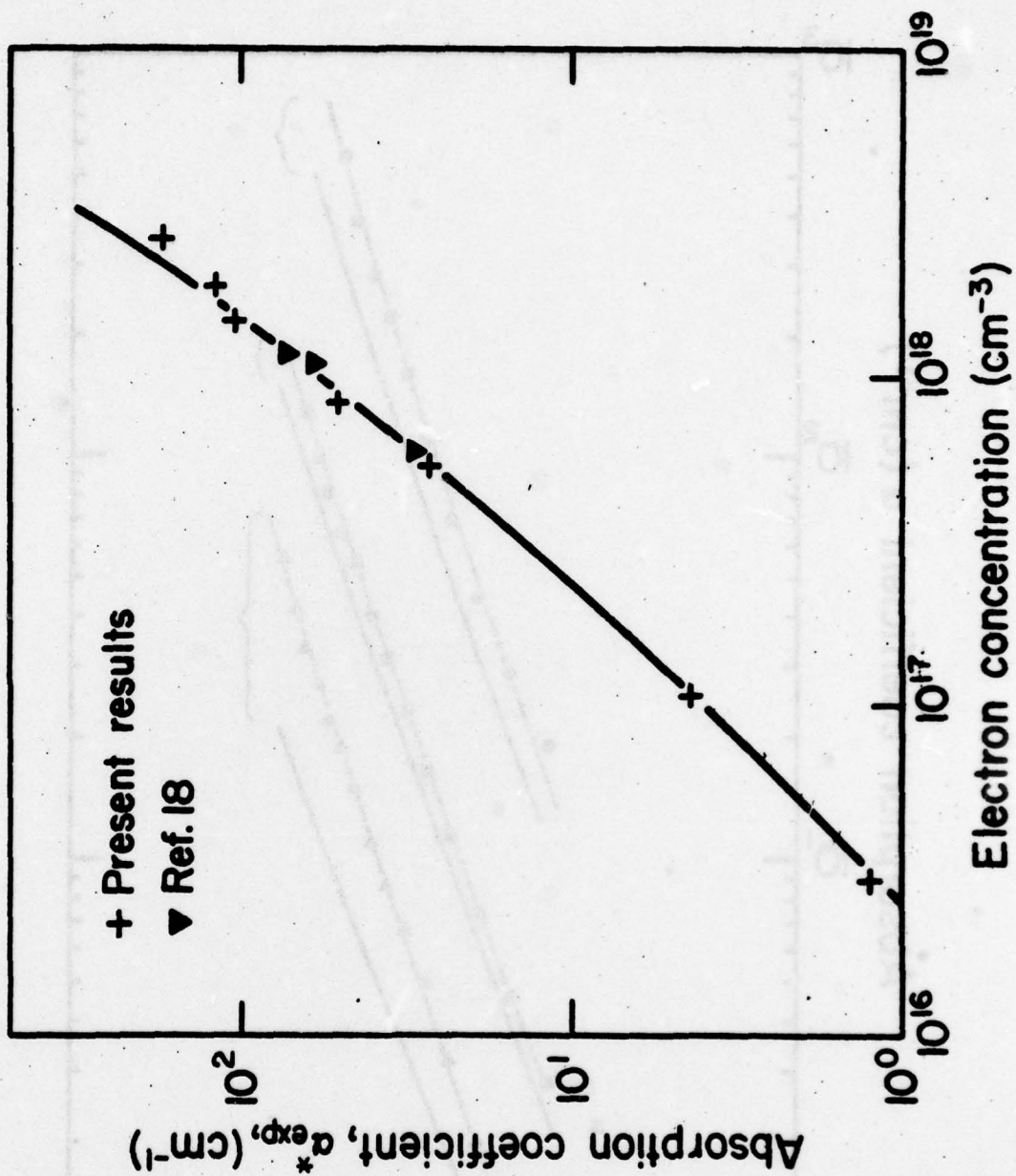


Figure 6



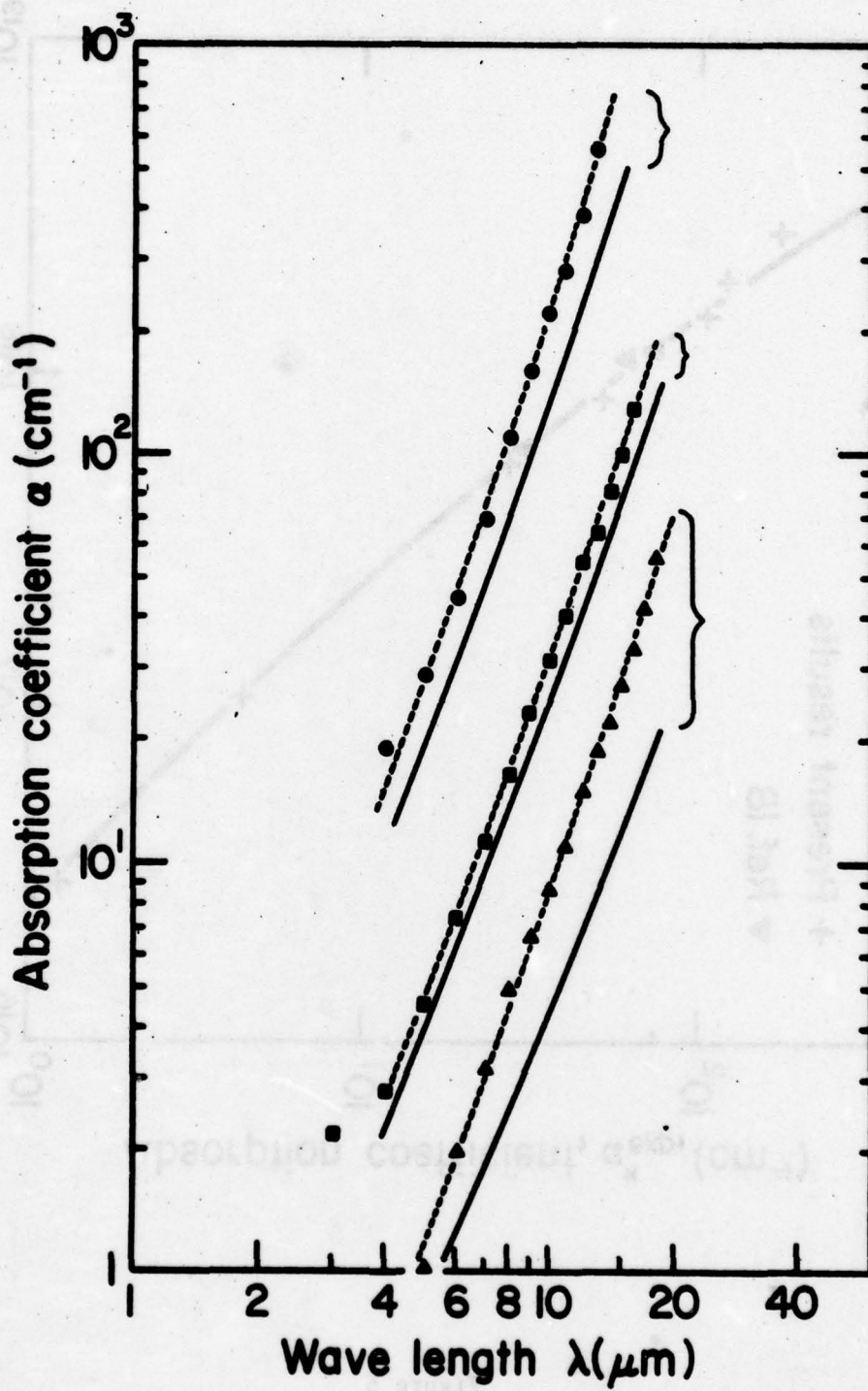


Figure 7

**MISSION**  
*of*  
**Rome Air Development Center**

*RADC plans and executes research, development, test and selected acquisition programs in support of Command, Control Communications and Intelligence (C<sup>3</sup>I) activities. Technical and engineering support within areas of technical competence is provided to ESD Program Offices (POs) and other ESD elements. The principal technical mission areas are communications, electromagnetic guidance and control, surveillance of ground and aerospace objects, intelligence data collection and handling, information system technology, ionospheric propagation, solid state sciences, microwave physics and electronic reliability, maintainability and compatibility.*

Printed by  
United States Air Force  
Hanscom AFB, Mass. 01731